Chemically Driven Convection in the Belousov-Zhabotinsky Reaction
—Evolutionary Pattern Dynamics—

Hidetoshi Miike[1*], Tatsunari Sakurai[2], Atsushi Nomura[3] and Stefan C. Müller[4]

[1]*Organization for Research Initiatives, Yamaguchi University, 1677-1, Yoshida, Yamaguchi, Japan*
[2]*Faculty of Science, Chiba University, 1-33, Yayoi-cho, Inage, Chiba, Japan*
[3]*Faculty of Education, Yamaguchi University, 1677-1, Yoshida, Yamaguchi, Japan*
[4]*Institute for Experimental Physics, Otto-von-Guericke University Magdeburg, Universitätsplatz 2, D-39106 Magdeburg, Germany*
E-mail address: miike@yamaguchi-u.ac.jp

In this work we review recent developments of experimental studies on chemically driven convection (CDC) emerging in a thin solution layer of the Belousov-Zhabotinsky reaction. Firstly, there are solitary waves due to convections and oscillatory or rotating convections accompanied by phase waves leading to global flow-pattern dynamics (called "flow waves"). The mechanism to realize the coherency and/or synchrony of such hydrodynamic patterns has not been established yet. Secondly, we summarize several models explaining some of these dynamics and show problems of the models. Especially, we emphasize the role of synchrony among nonlinear oscillators to establish hierarchical pattern dynamics of chemical wave trains and the flow waves. Thirdly, we demonstrate several examples of evolutionary pattern dynamics induced by CDCs in a batch reactor. In the reactor, the emerging phenomena show temporal development and evolutionary pattern dynamics. The direction of this development is from simple to complex, which looks like an evolution emerging in a real *reaction-diffusion-convection* system.
Key words: Chemical Wave, BZ-Reaction, Convection, Flow Waves

1. Introduction

It is already more than 10 years ago that Strogatz summarized a grandiose theory of the emerging science of spontaneous order in his book "SYNC" (Strogatz, 2003). Following the pioneering work of Winfree (1987), Kuramoto and Haken (1980) and other eminent scientists, he made important contributions to develop the field of nonlinear science. During the last half century, every decade or so, such grandiose theories came along. These are cybernetics (in the 1960s), catastrophe theory (in the '70s), chaos (in the '80s) and complexity theory (in the '90s). The ominous sounding C-names (beginning with a C) were followed by an E-name (Emerging Science) in the first decade of our new century. Nowadays, as is correctly pointed out by Strogatz (2003), "*Even the most hard-boiled, mainstream scientists are beginning to acknowledge that reductionism may not be powerful enough to solve all the great mysteries we're facing*". The mysteries on the problems of the 21st century are the origin of life, the function of cell, cancer, consciousness, AIDS, global warming, and many others. He also asserted: "*In such cases, the whole is surly not equal to the sum of the parts. These phenomena, like most others in the universe, are fundamentally nonlinear. That's why nonlinear dynamics is central to the future science.*" In the 2010s, we do not yet recognize the next grandiose theory in this field. As a sub-purpose of this review, we are just trying to seek for a candidate name of the next theory in this field.

Chemical waves of excitation in the Belousov-Zhabotinsky (BZ) reaction are a thoroughly studied example of dynamic pattern formation in the field of nonlinear science. Propagation of wave fronts through space is predominantly based on the molecular diffusion of an autocatalytic chemical species which results in local coupling to the neighborhood of the front. Thus, the BZ reaction is a representative example of a "*reaction-diffusion*" system. A variety of pattern dynamics have been reported for phenomena in a thin solution layer of this reaction. These are target patterns, rotating spirals and more complex patterns (Field and Burger, 1985; Kapral and Showalter, 1994). Usually, when we trigger the spiral waves in the solution, the pattern dynamics continues for more than 30 minutes. During this time period, the system is considered to stay in a quasi-stationary state. However, the system is changing in the course of time because of the consumption of a material providing an energy source (malonic acid) and reaction products (CO_2 and bromomalonic acid). Strictly speaking, in this sense the system is not under a stationary state. Many scientists like Castets *et al.* (1990) and De Kepper *et al.* (1991) developed a gel system with a combination of continuously fed unstirred open reactors to realize a stationary state. A gel system was used to realize an ideal "*reaction-diffusion*" model without convection. The flow rate of the open reactor controls the "distance" to non-equilibrium. The convection, usually associated with the chemical reaction and evaporative cooling of the solution surface, can be suppressed in such a gel system.
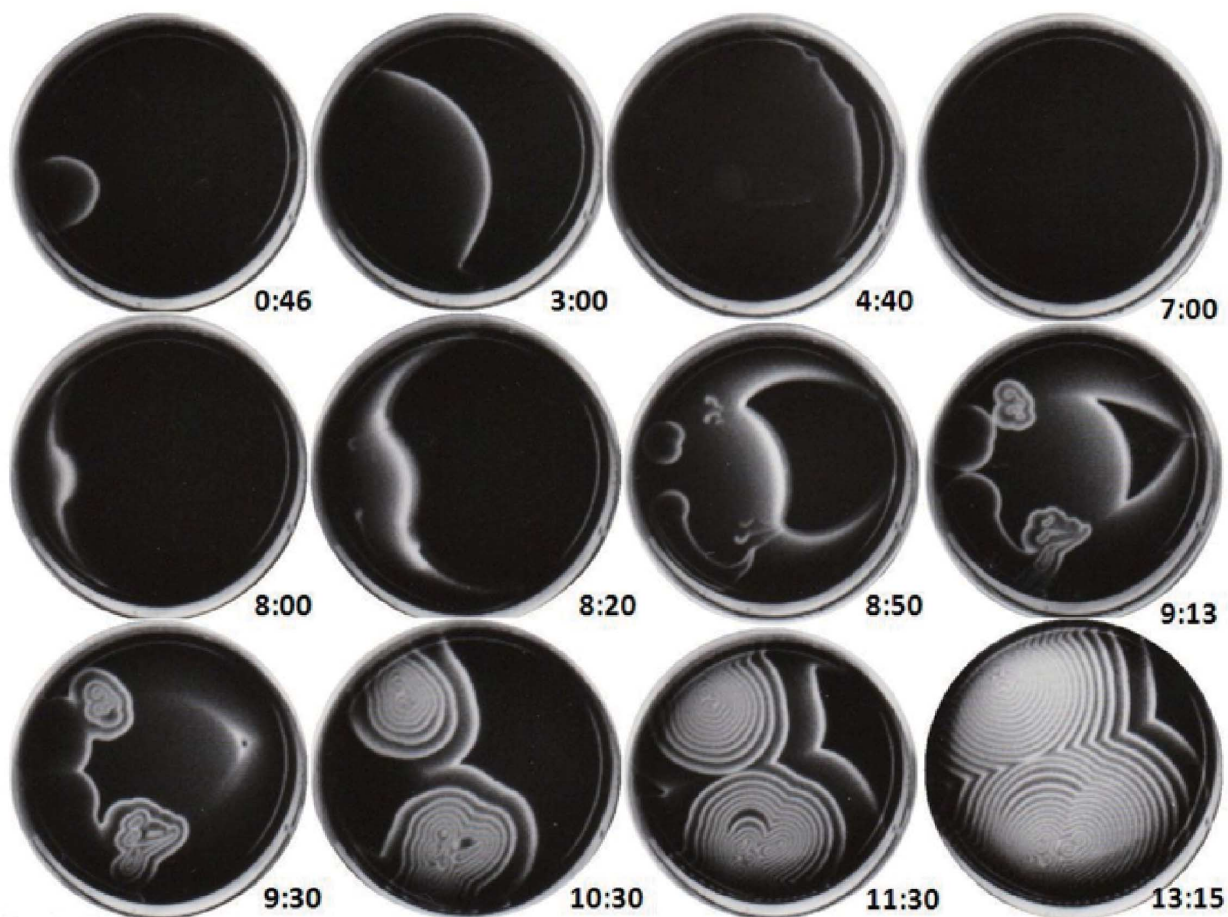
Fig. 1. Successive pattern dynamics coupled with chemically driven convections in a thin solution layer (depth 0.85 mm) of the BZ-reaction (Miike *et al.*, 1992).

With this system, our understanding has progressed far in the pattern dynamics of a "*reaction-diffusion*" model under a stationary state far from equilibrium. In our research, however, understanding the stationary or time-dependent non-linear dynamics of the "*reaction-diffusion*" system is not the final goal. A significant goal of science is to understand evanescent phenomena like birth, growth, death, regeneration and evolution emerging in a real complex system. Trying to understand such complex phenomena, we extended the frame of "*reaction-diffusion*" systems by considering convection as an additional transport process, thus dealing with "reaction-diffusion-convection" systems in our research objectives.

Frequently, there occurs an additional spatial transport process, which is hydrodynamic convection caused by concentration dependent surface tension changes around the location of the traveling front. The flow has a significant influence on wave speed and wave geometry including turbulent wave decomposition and global synchronization effects (Agladze *et al.*, 1984; Miike *et al.*, 1988, 1993, 2010; Pojman and Epstein, 1990; Pojman *et al.*, 1991; Kai *et al.*, 1993; Matthiessen and Müller, 1995; Matthiessen *et al.*, 1996; Diewald *et al.*, 1996; Sakurai *et al.*, 1997a, 1997b, 2003, 2004; Miike and Sakurai, 2003; Mahara *et al.*, 2009). As the main purpose of this article, we present an overview of observations in these complex patterns and attempt to ex-

plain a number of characteristic features in the framework of a "*reaction-diffusion-convection*" model.

Figure 1 shows a remarkable picture sequence, which represents the richness of the pattern dynamics that can appear in a *reaction-diffusion-convection system* (Miike *et al.*, 1992). In a thin solution layer of BZ-reaction, we found a successive pattern dynamics of chemical waves accompanied by chemically driven convections (hereafter abbreviated as CDCs). The successive transitions show almost all the varieties of CDCs in a typical experiment. A single chemical wave was triggered by a silver wire at time $t = 0$ min. The first wave propagated with almost constant speed. The propagation took about 5 minutes after the initiation. The second wave was induced spontaneously at around 7:40 min and propagated in an accelerating fashion. This wave is known as the "big wave" accompanied by a vigorous convection with turbulence. The propagation took only 1:30 min. Because of the turbulence, the chemical wave front was disturbed (at 8:50 min) and spiral waves were formed after the big wave propagation. Namely, by just triggering one chemical wave in the dish, three types of chemical waves with different CDCs appeared successively in a self-organized manner. These are an ordinary chemical wave having almost constant propagation speed (0:46–7:00 min), the "big wave" with accelerating propagation (8:00–9:13 min), and spiral waves induced by a vigorous convec-
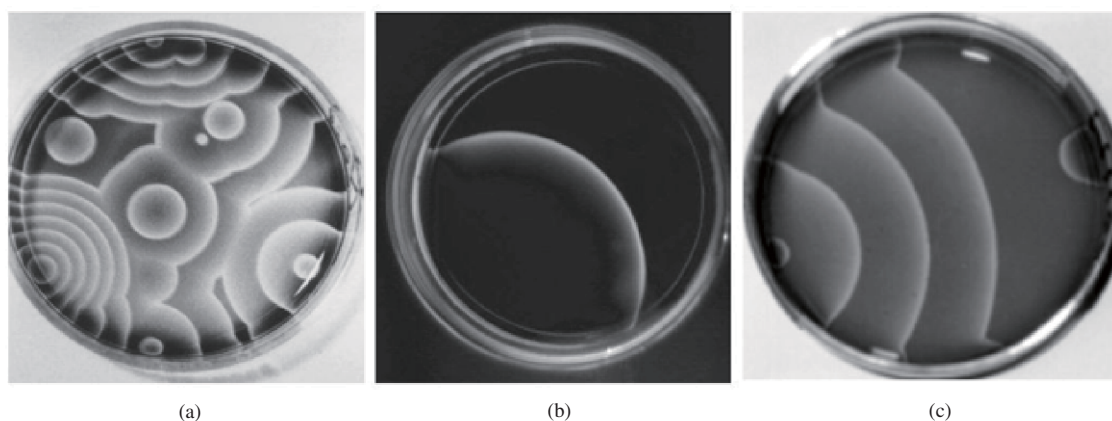
Fig. 2. (a) Target patterns of chemical activity under uncontrolled condition, (b) and (c) single circular wave and a target pattern, respectively, under well controlled condition (Castets *et al.*, 1990; Sakurai *et al.*, 1997b). Under such a condition, except for the triggered wave any spontaneous initiation of chemical waves is almost suppressed during the triggered wave propagation (see (b)) in the Petri dish (diameter 6.8 cm).
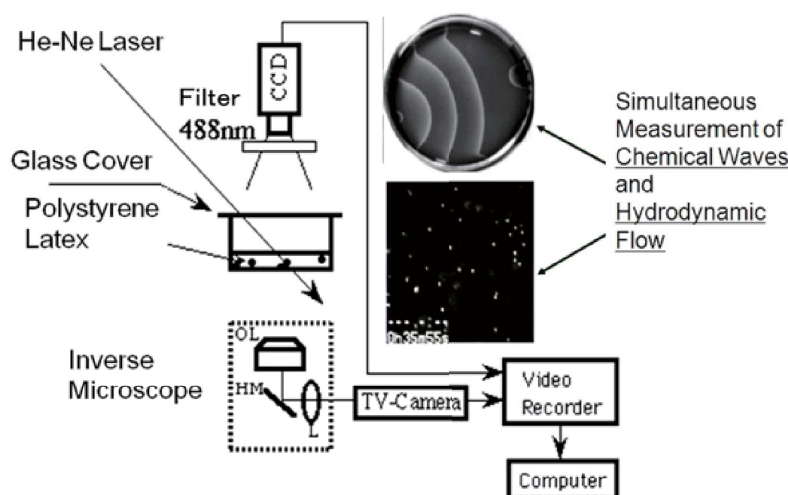

Fig. 3. Schematic diagram of the microscope video imaging system (Müller *et al.*, 1985; Miike *et al.*, 1992). Simultaneous measurement of chemical activity and hydrodynamic motion was realized.

tion caused by the big wave (9:30–13:15 min). Finally, a global flow wave emerges in a well-developed spiral structure. The successive dynamics could be a typical example of an evanescent and/or evolutional phenomenon, which we have reported already in 1991, at the workshop on "Pattern Formation in Complex Dissipative Systems" (1991, Kitakyushu, Japan) (Miike *et al.*, 1992). Details of the pattern dynamics and a related discussion will be presented in Sections 5 and 6.

2. Experimental Methods

2.1 A recipe of the BZ-solution for measuring chemically driven convection

Experiments were carried out in an excitable BZ-solution catalyzed by ferroin in a batch reactor (Petri dish, diameter 7–15 cm) at a room temperature of about 25°C. The BZ-solution was obtained by preparing a mixture of 48 mM sodium bromide, 340 mM sodium bromate, 95 mM malonic acid, and 378 mM sulfuric acid. About 5 minutes after mixing, the catalyst and indicator ferroin (3.3 mM) was added.

For the purpose of the experiment, polystyrene particles (diameter, 0.48 μm) serving as scattering centers were mixed into the solution. With the small amount (about 10^6 particles/ml) of polystyrene almost no effect on the pattern evolution was found. The mixture was filled into a Petri dish to a depth of about 0.85 mm at the center of the dish. Experiments were carried out with covering the sample dish with a glass plate. The procedure for triggering a chemical wave is described in Miike *et al.* (1988). An air gap of about 12 mm was left between the layer surface and the glass cover. Fresh samples were prepared for each experiment. Experiments were started (time = 0:00 min) soon after triggering the chemical waves in the solution.

2.2 A method suppressing any spontaneous excitation of a chemical wave and producing a minimum nucleation of CO_2 bubbles

In a non-stirred batch reactor of the BZ-solution, we often observe many spontaneous excitations of chemical waves under usual experimental conditions. These are target patterns and/or spiral waves (see Fig. 2(a)). Under these
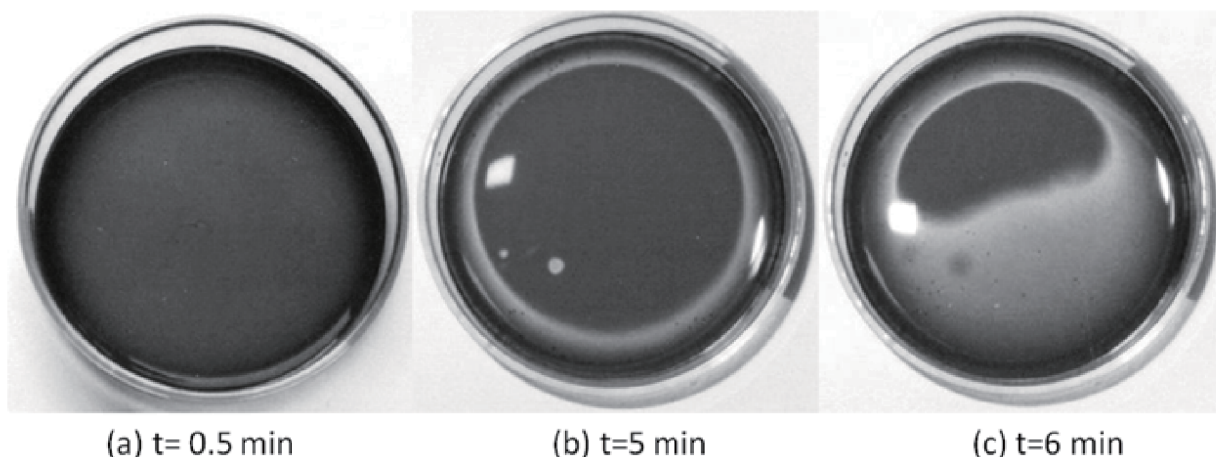
Fig. 4. Relaxation process to a well reduced state of the BZ solution. After the reduction of the solution, a "kinematic wave" propagated with high speed. There is almost no spontaneous induction of chemical waves during the reduction stage (0–5 min).

incoherent conditions of chemical waves, it is hard to observe convective flow associated with the chemical waves. One exception is a convective structure caused by evaporative cooling under the condition that the cover of the Petri dish is removed. A static pattern of the convection roll appears within about 3 minutes after removing the cover from the dish. This convective structure (a "mosaic" pattern) is not caused by chemical waves, which merely serve to visualize pre-existing hydrodynamic currents (Borckmans and Dewel, 1988). The convective pattern can be suppressed by covering the top of the dish to prevent evaporation. In this study, all the experiments were carried out under the condition that the top of the dish was covered by a glass plate but left an air gap of about 12 mm between the cover and the solution surface to keep free liquid-air interface conditions (Miike and Sakurai, 2003; Miike *et al.*, 2010).

If we carry out a careful treatment of the dish (Sakurai *et al.*, 1997b), we can suppress any spontaneous excitation of chemical waves and realize a minimum nucleation of CO_2 bubbles. Thus we can control chemical wave initiation and create a coherent structure of chemical waves (see Figs. 2(b) and (c)). Only under this "clean" condition, we succeeded to observe coherent pattern dynamics of convective flows induced by a chemical wave itself. A detailed treatment to realize the "clean" condition is as follows:

(1) Use distilled and ion-exchanged pure water in the preparation of BZ reagents.

(2) Prepare a scratch-free and dust-free Petri dish.

(3) Keep hydrophilic condition of the inner surface of the dish before each experiment by filling the dish with the pure water.

2.3 Measuring system

Simultaneous observations of chemical activity and hydrodynamic phenomena were carried out by a microscope video imaging system (Müller *et al.*, 1985; Miike *et al.*, 1992). To visualize hydrodynamic flow in the BZ-solution, laser light illumination and polystyrene particles were introduced. The system consisted of a He-Ne laser (632.8 nm), an inverted microscope, a TV-camera, a video recorder and a personal computer. A schematic diagram is given in Fig.

3. Polystyrene particles were illuminated by a He-Ne laser light to trace the hydrodynamic motion. The motion of the particles was measured using the TV camera and a video recorder. Automatic measurement of the flow velocity is done by TV-camera, video recorder and personal computer (Müller *et al.*, 1985; Miike *et al.*, 1987, 1992). Spatial filtering velocity measurement based on image sequence processing (Miike *et al.*, 1987) was adopted to analyze the temporal traces of the particle velocity.

3. Solitary Convection Associated with Single or Discrete Chemical Waves

3.1 First evidence for chemically driven convection in the BZ solution

After mixing the reacting solutions in a cuvette, the BZ solution is poured into the Petri dish. Usually, the solution is suddenly once oxidized (change to blue color) and is reduced gradually with time (becomes red again). If we carry out careful treatment of the dish as described above, there is no spontaneous induction of chemical waves and almost no nucleation of CO_2 bubbles (see Fig. 4(a)) during the reducing time stage. At about 5–6 minutes after mixing the BZ solution an oxidized region (blue color) appears in the outskirts of the dish (see Fig. 4(b)), and a rapid propagation of a "kinematic wave" often follows. Since the adopted BZ solution (Miike and Sakurai, 2003) can be regarded as an oscillatory system having a long oscillation period (about 5–8 minutes), the kinematic wave is considered as a phase wave and/or phase diffusion wave. On the other hand, we can excite trigger waves such as circular waves and spiral waves manually by use of a silver wire during the reducing stage of the BZ solution. Thus we have various types of chemical waves in the BZ-solution. In this chapter we focus on intrinsic convections induced by these waves in a thin BZ solution layer. Here we refer to hydrodynamic phenomena induced by the kinematic wave in a batch reactor of the BZ solution representing the first evidence of chemically driven convection (CDC).

As described above, if we do not disturb the system, no spontaneous initiation of chemical wave is observed dur-
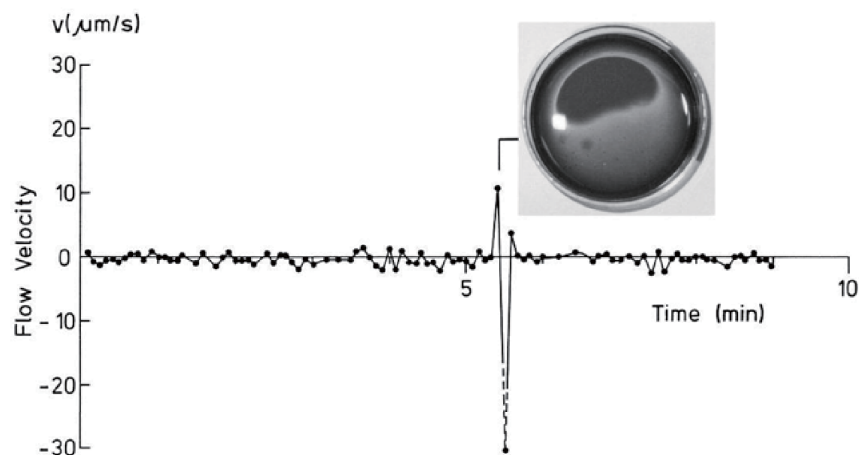
Fig. 5. Evidence of CDC caused by the kinematic wave propagation. A sudden change of the hydrodynamic flow velocity was detected at about 6 minutes after pouring the BZ-solution into a Petri dish. Flow velocity was evaluated manually by the motion of small dust particles (diameter less than 0.5 mm) on the surface of the solution.
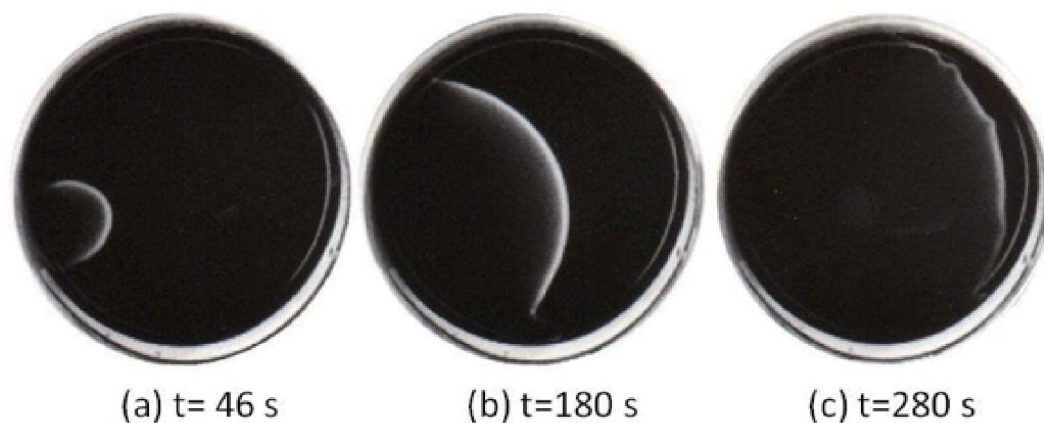

Fig. 6. Temporal development of a single propagating wave. No initiation of the uncontrolled waves is kept during the wave propagation. The "clean" condition is essential to observe the chemically driven convection (CDC). The diameter of the dish is 6.8 cm.

ing the reducing stage (see Fig. 4(a)) under well controlled conditions. No remarkable hydrodynamic flow is observed during this stage (see Fig. 5). At about 5–6 minutes after mixing the solution an oxidized region (blue color) appears in the outskirts of the dish and rapid propagation of a "kinematic wave" often follows (Fig. 4(c)). A sudden change of the flow velocity occurred at about 6 minutes after pouring the BZ-solution into the dish (see Fig. 5). The corresponding photograph is shown in the figure, which indicates that the kinematic wave causes a sudden change of the flow velocity. Since the observation was not continuous, it was difficult to estimate correctly the maximum amplitude of the flow velocity. The solution layer returned to a resting state after the kinematic wave had passed by (after 7 minutes in Fig. 5).

3.2 Solitary convection caused by an ordinary triggered chemical wave

Direct observation of Convection caused by a triggered chemical wave was observed directly, and an oscillatory hy-

drodynamic flow in spiral waves of the BZ reaction was found (Miike et al., 1988). The details of the oscillatory flow are discussed in Section 4. To clarify the mechanism of these flow oscillations we carried out simpler experiments of CDC with a single circular wave (see Fig. 2(b)), while suppressing evaporation from the surface of the BZ-solution layer (Miike et al., 1988; Miike and Sakurai, 2003). Figure 6 shows the propagation of such a single wave triggered in a thin layer with a depth of 0.85 mm. No initiation of the uncontrolled waves occurred during the observation time. If many waves are triggered spontaneously in the dish, many origins of CDC serve as counter balances, which cannot create any directional flow field. We recorded continuously the horizontal velocity component of the convective flow induced by the wave. The result is shown in Fig. 7. Although the wave was triggered at the lower-left boundary of the dish, the hydrodynamic flow started immediately after the wave incitation. The flow direction pointed toward the wave front approaching the observation area (al-
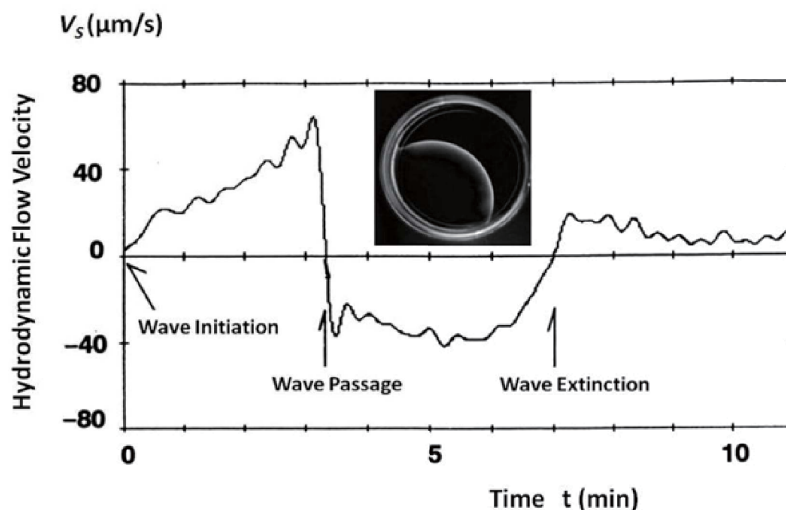
Fig. 7. Temporal trace of convective flows associated with single circular wave propagation. The chemical wave propagation causes a gradual increase of hydrodynamic velocity observed at the middle of the Petri dish (Miike *et al.*, 1988; Miike and Sakurai, 2003).
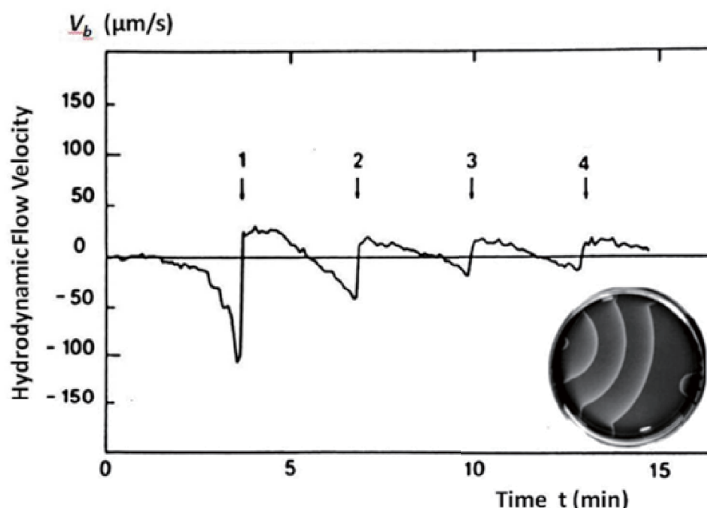

Fig. 8. Time trace of the flow velocity V_b measured near the bottom of the solution at the middle of the dish. Discrete chemical waves (numbered 1, 2, 3, and 4) of the "target pattern" are induced spontaneously by triggering a single circular wave at the left end of the dish (see the picture) (Miike *et al.*, 1988; Miike and Müller, 1990; Miike and Sakurai, 2003). The direction of chemical wave propagation coincides with that of negative flow velocity. The flow velocity measured near the surface V_s has a larger amplitude and opposite direction.

most at the middle of the Petri dish). We defined this direction to be positive in the figure. The surface flow velocity V_s changed its direction suddenly after the passage of the chemical wave at about 3 minutes. The sudden change of direction is similar to that in the kinematic wave (see Fig. 5); however, the change has a rather gentle slope. After extinction of the wave at the opposite boundary of the dish (upper right side: see Fig. 6(c)), the flow changes its direction again at about 7 minutes and its amplitude decreases with time. These results provide an important clue for constructing a global structure of the convective flow in the BZ-solution.

Figure 8 shows the hydrodynamic motion induced by a target pattern (see Fig. 2(c)). When the wavelength between successive circular waves is large enough (let us say 10 mm), the passage of each wave induces a clear hydrody-namic motion (a kind of flow oscillations). There occurs a directional flow near the solution surface. The flow velocity near the surface V_s first points to the wave front and the velocity increases, as the front approaches the fixed observation area. After wave passage, the surface flow suddenly reverses its direction. By contrast, the direction of hydrodynamic flow near the bottom V_b shows the opposite behavior as shown in Fig. 8. There, the direction of wave propagation coincides with that of positive flow velocity. These results corroborate the existence of propagating convection rolls accompanied by the chemical wave propagation (Miike and Sakurai, 2003; Miike *et al.*, 2010). The behavior of the target pattern is similar to that of the single wave. Important points are the following: As the number of passing chemical waves increases, the amplitude of the flow change decreases at a fixed observation point (almost the middle of

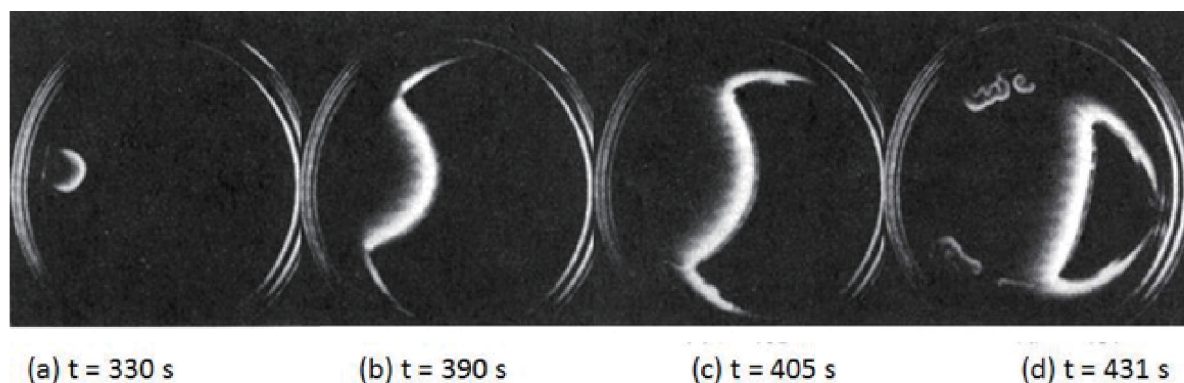(a) t = 330 s   (b) t = 390 s   (c) t = 405 s   (d) t = 431 s

Fig. 9. Front propagation of a big wave triggered at time $t = 300$ s after mixing the catalyst to the BZ solution (Miike *et al.*, 1993). The propagation across the Petri dish takes only about 100 seconds, which is almost one third of the duration required by the ordinary wave shown in Fig. 6. The accelerating nature of the propagation depends on the triggering time after mixing the solution (Fig. 10).
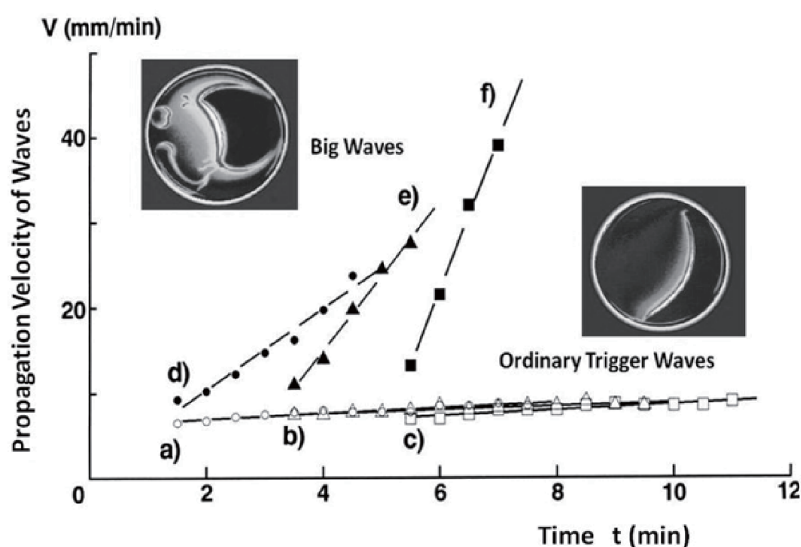

Fig. 10. Time evolution of propagation velocity of chemical waves (Miike *et al.*, 1993). a) ◯, b) △, and c) ☐ ordinary waves are triggered at $t = 1, 3$, and 5 min after mixing the BZ-solution, respectively. d) ●, e) ▲, and f) ■: big waves are triggered at $t = 1, 3$, and 5 min, respectively.

the dish); the amplitude of the flow depends on the wavelength of the target pattern.

From the above results of the discrete wave experiments (including kinematic waves, single chemical wave fronts and target patterns), one can summarize:

1) Chemical waves induce convection in a thin layer of BZ solution.

2) The convection rolls propagate with the waves, which produces a kind of hydrodynamic flow oscillation, when observed at a fixed point.

3) Periodic passage of the waves results in a periodic change of the hydrodynamic flow direction.

3.3   Vigorous and destructive convection induced by a "big wave" with enhanced chemical activity

When the onset of a circular wave is triggered, a constant propagation velocity of chemical activity is observed, characterized by a pronounced but limited hydrodynamic effect (see Fig. 7). In extreme cases, however, rapid and accelerating wave propagation occurs in the BZ solution layer, as shown in the picture sequence of Fig. 9. The pronounced

reactive front was first reported as a "big wave" in the workshop on "Pattern Formation in Complex Dissipative Systems" (1991, Kitakyushu, Japan) (Miike *et al.*, 1992). Temporal traces of the propagation velocity of chemical waves can be seen in Fig. 10. The experimental conditions for the respective observations were kept almost the same. The ordinary trigger waves have a weak acceleration; however, the acceleration does not depend on the triggering time. In contrast, the "big waves" show a strong acceleration, and the acceleration does depend on the instant of the triggering time. Figure 11 presents a comparison of the CDC between the ordinary chemical wave (a) and the big wave (b, c). The ordinary wave propagates with an almost constant velocity and induces a weak convection velocity, which is usually less than 100 μm/s. On the other hand, the big wave produces vigorous convection. The flow velocity of the convection depends also on the triggering time. The higher the instant of triggering time delay, the more the velocity increases. In an extreme case, the maximum flow velocity (about 3000 μm/s) induced by the big wave is almost 30
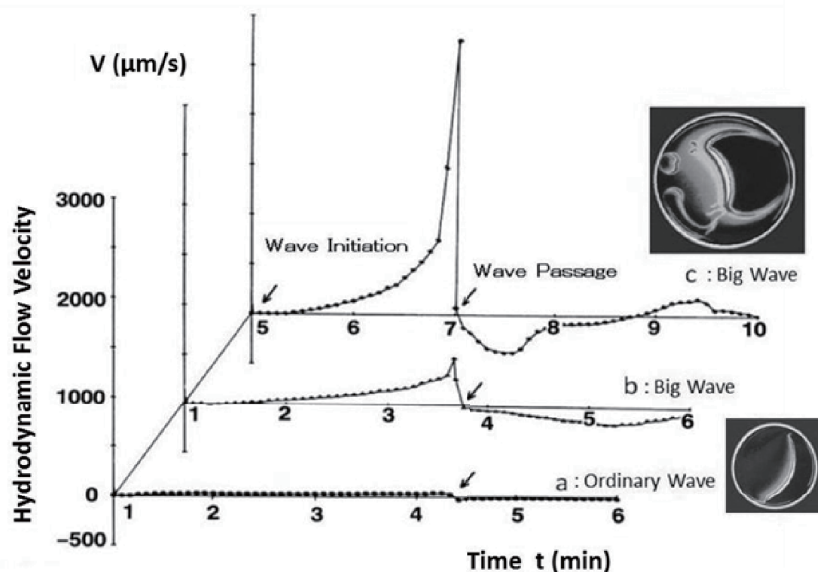
Fig. 11. Temporal traces of convective flow velocities induced by the ordinary chemical wave (a) and by the big waves (b, c) (Miike *et al.*, 1993).
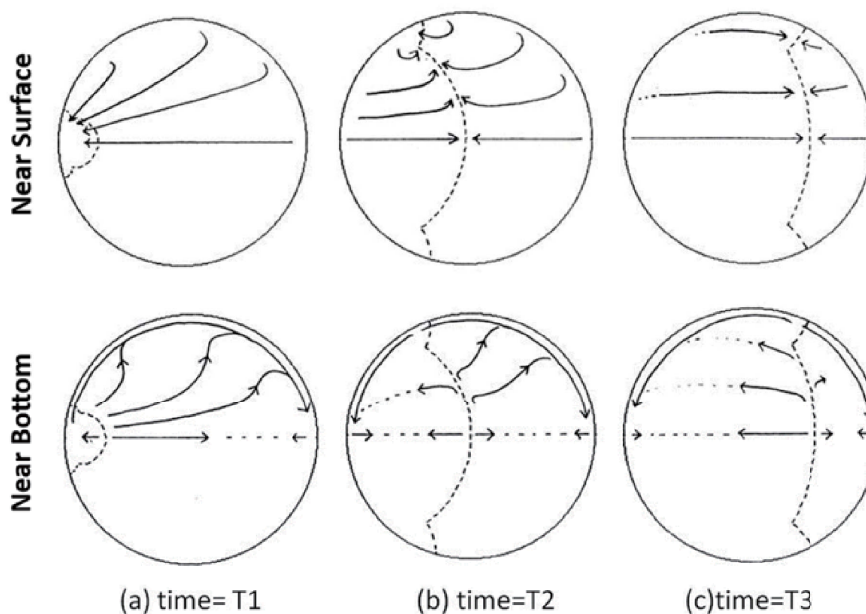

Fig. 12. Estimated horizontal flow structures based on repeated velocity measurement at many points of the Petri dish (Hashimoto *et al.*, 1991). Apparently, the single chemical wave propagation is accompanied by a propagating flow structure with a strong peripheral current near the bottom of the circular dish. The current is related to a larger propagation velocity of the big wave at the periphery of the dish (see Fig. 9).

times faster than that induced by the ordinary wave. Some remarkable characteristics of the big wave are:

(1) Broad and big oxidized front region having about 1 cm width (see Figs. 9(b) and (c)).

(2) Rapid propagation of the wave with accelerating speed depending on the triggering time (see Fig. 10).

(3) Pronounced velocity of the induced convection. The flow velocity can be almost 30 times faster than that of an ordinary wave (see Fig. 11).

(4) Spontaneous formation of a spiral structure induced by a well-developed big wave. When the pronounced velocity is large enough to destroy the chemical wave shape,

spiral structures appear in the wake of the wave which has just passed (see Fig. 9(d)).

Inomoto *et al.* reported that the transition from an ordinary trigger wave to the big wave depends on a concentration change of bromomalonic acid (BrMA), an important product of the BZ reaction. The authors suggested that the strong surface activity of BrMA was responsible for the transition (Inomoto *et al.*, 2000). Several authors tried to explain the acceleration by coupling the surface tension driven convection with the *reaction-diffusion* mechanism for chemical waves, such as the extended Oregonator model. The accelerating nature and accompanying vigorous

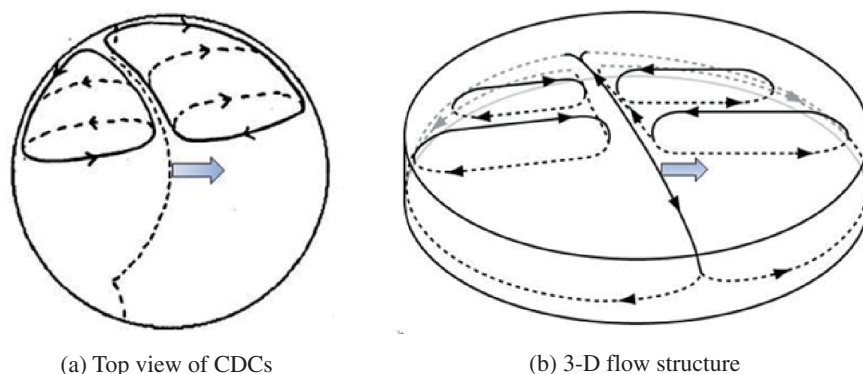(a) Top view of CDCs   (b) 3-D flow structure

Fig. 13.   A schematic model for the three-dimensional flow structure of CDCs induced by a single chemical wave (see Fig. 6). The broken line in (a) shows the front of chemical activity, and grayish large arrows show its propagating direction. Solid lines with an arrow in (b) indicate the hydrodynamic flows near the surface of the BZ-solution. Dashed lines with arrows show the flows near the bottom of the solution (Hashimoto *et al.*, 1991).
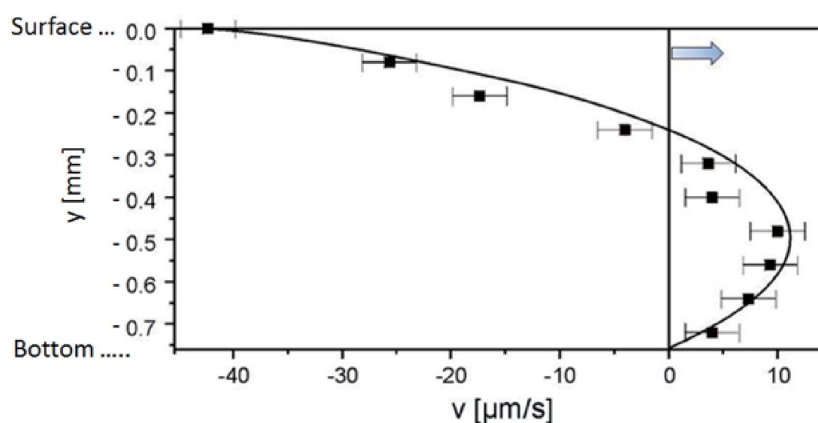

Fig. 14.   Comparison between experiments (rectangles with error bar) and simulation (solid curve) for the velocity profile $v(y)$ of convection induced by a single chemical wave. The grayish large arrow indicates the propagation direction of the chemical wave (Matthiessen *et al.*, 1996).

convection of the big wave, however, are difficult to explain within the framework of an ordinary "*reaction-diffusion-convection*" scheme. We will summarize and discuss details of this problem in Section 6.

3.4 Horizontal structure and vertical profile of CDC induced by a single chemical wave

The experimental results discussed above are based on a local measurement of CDC. For better understanding the dynamic phenomena, global horizontal structures and vertical profiles of CDC were investigated. Figure 12 shows estimated horizontal flow structures based on repeated velocity measurement at many points in the system under consideration (Hashimoto *et al.*, 1991). From these results, we confirm that the single chemical wave propagation is accompanied by a propagating convective flow structure. A peculiarity of the flow structure is the existence of a strong peripheral current near the bottom of the circular dish. Hashimoto *et al.* (1991) suggested two types of flows:

1) Vertical downward flow at the front region of the chemical wave.

2) Horizontal flows toward the circumference of the Petri dish along the wave front.

The authors also proposed a three-dimensional structure of

the flow as shown in Fig. 13 (Hashimoto *et al.*, 1991), and suggested that the flow structure is dependent on the shape of the dish.

Several experimental and theoretical approaches have been presented to clarify the mechanism of CDCs in the BZ-solution. In an experimental approach, Yoshikawa *et al.* (1993) found direct evidence of thermocapillary forces of the chemical reaction by measuring periodic change of the surface tension in a continuously stirred BZ reaction. They suggested that the difference in surface tension between the two states of the iron-catalyst $[Fe(phen)3]^{3+}$ and $[Fe(phen)3]^{2+}$ was the driving force of the rhythmic phenomena. Thus, concentration gradients of the iron-catalyst at the wave front could be a driving force of the convective flow. A first quantitative explanation for the convective flow associated with chemical waves was proposed by Matthiessen *et al.* (1996). The mechanism of the chemically driven convection was investigated with space-resolved velocimetry using a set-up similar to Fig. 3, and simulated numerically by solving a set of modified Oregonator model equations and the Navier-Stokes equations. This work showed that a surface tension-induced flow, especially the vertical flow profile, matches best the experimental findings
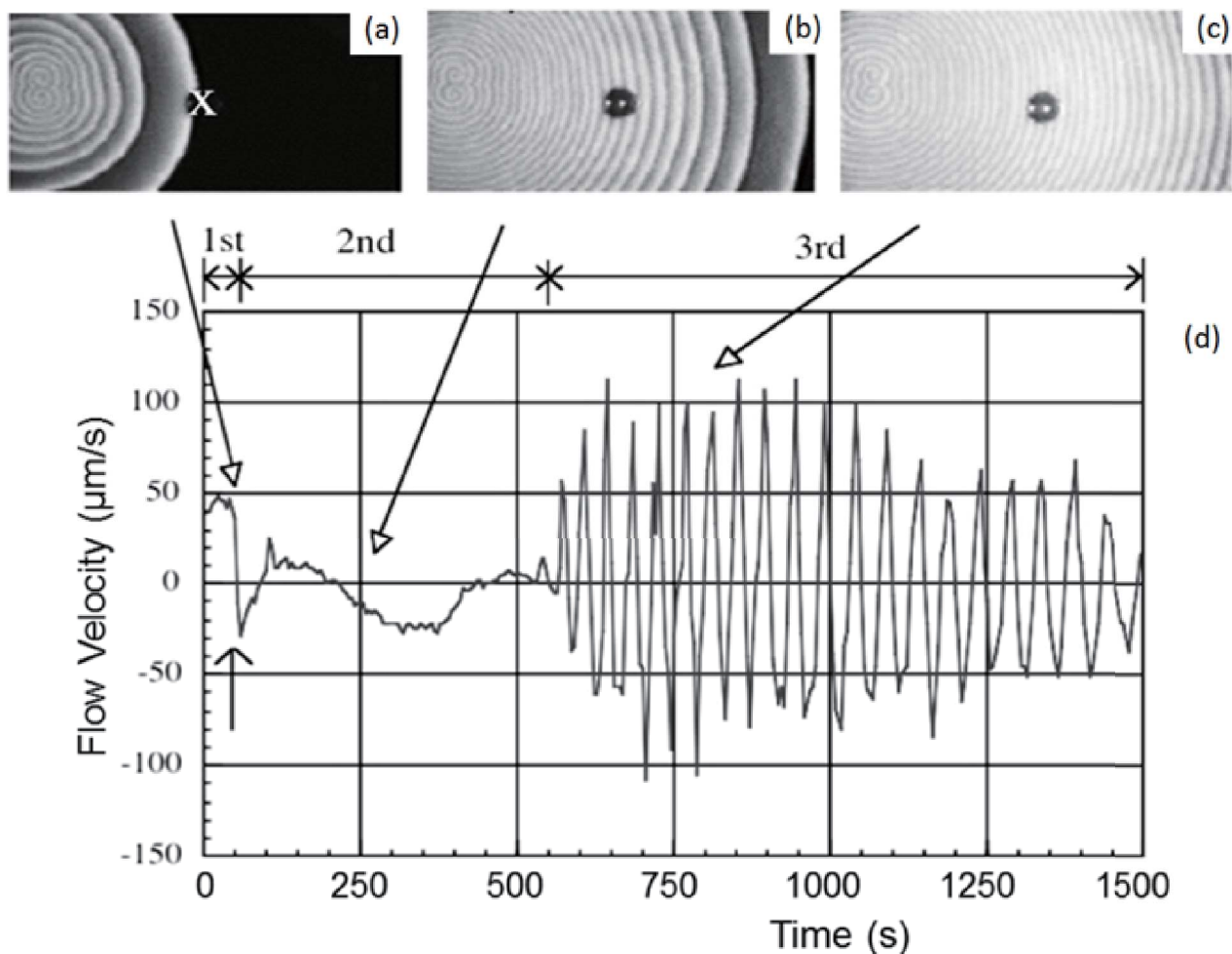
Fig. 15.   Development of chemical spiral waves ((a) to (c): one spiral pair (OSP)) and temporal evolution of the flow velocity (d) measured near the
surface of a BZ-solution layer at the center of a Petri dish (Sakurai *et al.*, 1997b). (a), (b), and (c) are image samples observed at about *t* = 50, 250,
and 800 s, respectively. The position marked x in (a) indicates the location of measurements of flow velocity. The oscillatory flow started in the third
stage after *t* = 550 s and continued for more than 1000 s.

in Matthiessen *et al.* (1996) (see Fig. 14). This result is the
only successful case of a theoretical approach at present.
Details of the model will be discussed in the following sub-
section (see 6.1).

4.   Oscillatory or Rotating Convection Induced by a Chemical Wave Train
4.1   Oscillatory convection caused by spiral waves: local flow structure

Figure 15(d) shows a temporal trace of hydrodynamic
flow velocity (Miike *et al.*, 1988; Sakurai *et al.*, 1997b) near
the surface of the BZ solution layer. The dynamic behavior
of the measured flow is separated roughly into three stages,
i.e., from *t* = 0 to 50 s, from *t* = 50 to 550 s, and from
t = 550 to 1500 s. In the first stage, when the first chemical
wave was approaching the observation area marked by (x)
in Fig. 15(a), the flow was directed toward the wave front.
We defined this direction, that is, from the observation point
to the spiral center, to be positive in Fig. 15(d). At about
t = 50 s the flow direction suddenly changed due to the
passage of the first wave in every experiment (see ↑ posi-
tion in Fig. 15(d)). The first discrete wave propagated into a

relatively well-reduced medium; therefore, the behavior of
the convective flow was similar to that of the flow induced
by an ordinary wave as shown in Fig. 7. In the second stage,
the distance between the wave fronts of the spiral wave train
decreased from 10 to 1 mm, as ten or more waves passed the
observation area (see Fig. 15(b)). Since the spiral wave train
propagated into a less reduced medium as compared to the
first stage (due to the shorter wavelength), the velocity of
the induced flow decreased with time. In this stage, there
was no correlation between the chemical wave passage and
the flow direction. After *t* = 550 s, however, the flow sud-
denly started to oscillate and developed a velocity of large
amplitude of flow (exceeding 100 μm/s). These oscillations
continued for more than 1000 s.

During this third stage, the flow oscillation is almost
synchronized or entrained with the periodic passage of the
chemical waves. We found that the period of flow oscilla-
tion (40–50 s) is almost twice the period of chemical wave
passage (20–25 s). The mechanism of the entrainment has
not yet been clarified. Since the Petri dish is a batch reactor,
the velocity amplitude decreased with time after *t* = 1000 s.
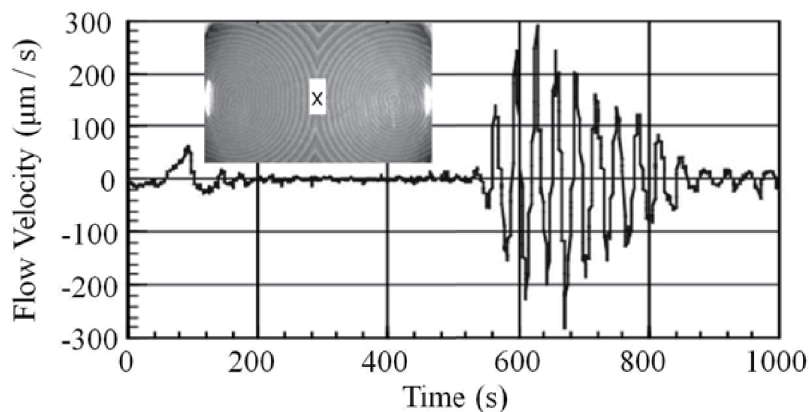Thus, we notice that the oscillation stage having almost con-

Fig. 16. Temporal evolution of the flow velocity associated with two spiral pairs (TSPs). The flow velocity was measured at the location x in the picture near the surface of a BZ solution layer at the center of the Petri dish (Sakurai *et al.*, 2004).
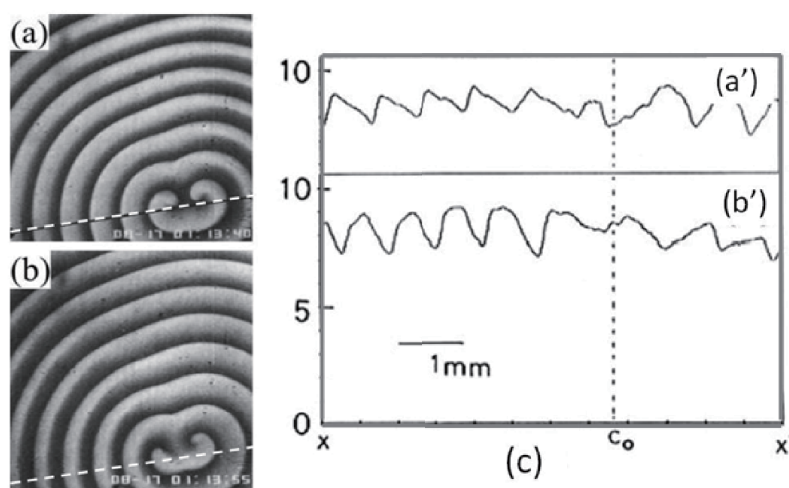

Fig. 17. Synchronous deformation of chemical wave profiles accompanied by the oscillatory flow (Miike *et al.*, 1988; Miike and Sakurai, 2003). Sectional brightness profiles along the tilted broken white line in (a) time = 13:40 (13 min and 40 s) from triggering the waves and (b) time = 13:55 are shown in (c). The sectional profiles in (a) and (b) correspond to the waves (a') and (b') in (c), respectively; C_0 is the center position of the chemical spiral wave.

stant amplitude can be regarded as a quasi-stationary state (650 < t < 1050).

Figure 16 shows another example of oscillatory flow induced by spiral waves. The convective flow velocity was traced near the surface of the solution at the middle of the Petri dish. When two spiral wave pairs are triggered symmetrically as shown by the picture in Fig. 16, oscillation of flow appears suddenly around t = 530 s after excitation of the spiral centers. The period of the flow oscillation is about 30 s. The maximum amplitude of the flow velocity is larger than 250 μm/s. The maximum velocity exceeds the propagating velocity of ordinary chemical waves (about 100 μm/s). The amplitude of the flow oscillation, however, decreases in the course of time. After a while, in some cases, the flow oscillation started again spontaneously in the same solution. The second oscillation has smaller amplitude and longer period in comparison with the first oscillation. Since our system is a batch reactor, the condition of the system changes with time.

Comparing the two systems with one spiral pair (OSP:

see Fig. 15) and two spiral pairs (TSPs: see Fig. 16), we notice that:

1) The period of incubation (P_i) for the flow oscillation is comparable, although [P_i(OSP) > P_i(TSPs)].

2) The maximum amplitude of flow oscillation (MA_o) is different, where [MA_o(OSP) < MA_o(TSPs)].

3) The duration of flow oscillations (D_o) is different, where [D_o(OSP) > D_o(TSPs)].

The above facts suggest differences in the energy dissipation rate and in the duration of a quasi-stationary state between two systems. If we can design an open system for this purpose to elucidate this possibility, we may encounter more coherent and rich pattern dynamics in the *reaction-diffusion-convection* system of the BZ-solution having a free liquid-air surface.

4.2 Hierarchical dynamics of flow waves: global flow structure in CDCs

In this section, we focus our attention on flow waves, which were found by Matthiessen and Müller (1995). They investigated a global structure of the flow oscillation and
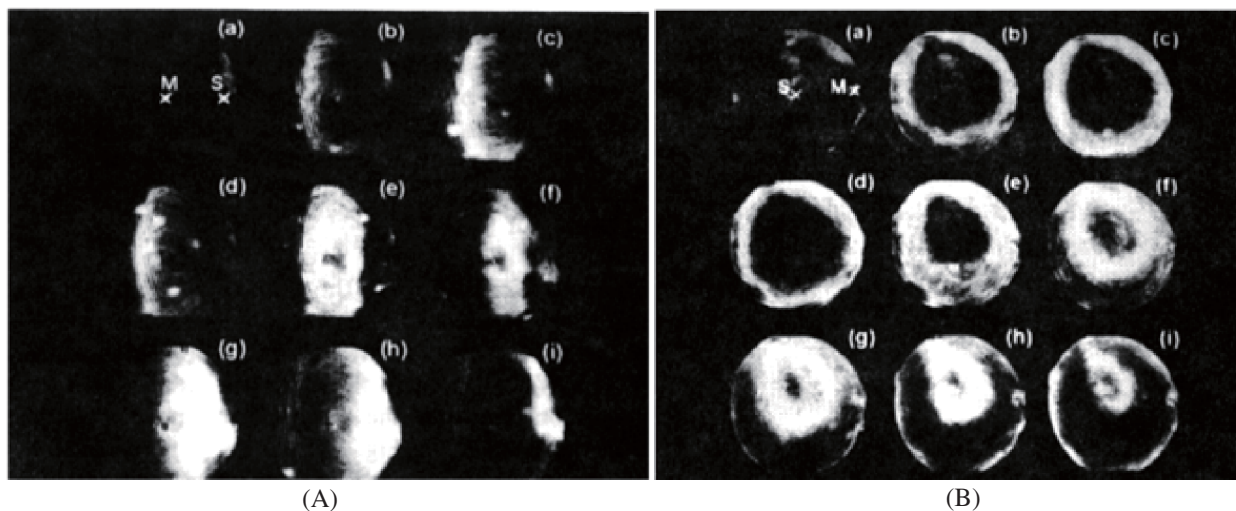
Fig. 18. Global views of the oscillatory flow in the systems with the spiral centers (at point S) near the right boundary in (A) and in the middle of the dish in (B). White bands (A) and white circular regions (B) show the flow waves, which propagate to the center of spiral waves. The images were obtained by background subtraction, smoothing, and contrast enhancement. The time delay between frames was 8.4 s. The points of flow measurement were located in points (M) (from Matthiessen and Müller (1995)).

found "flow waves" with a wavelength of the order of ten chemical waves traveling through the dish toward the center of chemical spiral waves. To visualize a global distribution of the flow direction, they utilized the deformation of chemical wave profiles by hydrodynamic flow (see Fig. 17) (Matthiessen and Müller, 1995). The concentration profile of a chemical wave traveling against the direction of surface flow differs slightly from that traveling in the direction of the flow.

The slight difference of brightness profiles of visualized patterns was enhanced by image processing. The result of the processing is shown in Fig. 18, in which the spiral centers were placed at the right boundary Fig. 18(A) and in the middle Fig. 18(B) of the dish (Matthiessen and Müller, 1995). The following observations were reported: a bright band appears in the second image (b) of Fig. 18(A), near the dish boundary. It moves toward the spiral center, and finally disappears. The bright band represents surface flow in the direction of chemical wave propagation. As the bright band shows a region with simultaneously tilted wave fronts, we can observe a global flow wave traveling through the dish toward the spiral center. Figure 18(B) depicts a similar situation. However, the spiral center was placed in the middle of the dish. Consequently, a flow wave with circular geometry appeared near the dish boundary. It moved toward the spiral center and finally disappeared there.

Figure 19 shows local structures near the point S in Fig. 18(A) more clearly, where visualized patterns were enhanced by a novel image processing procedure making use of a pixel-based temporal brightness enhancement (Miike *et al.*, 1999). Chemical wave activity and flow waves dynamics are visualized simultaneously. The brighter area surrounded by the black ellipse in Fig. 19(c) corresponds to white bands in Fig. 18(A). More than 20 waves of chemical activity are included in the flow wave propagation having the same brightness profiles. This finding suggests a synchronous deformation of the chemical wave profiles caused

by the oscillatory flow, which emerges in a well-developed coherent structure of a chemical spiral pattern (see Figs. 19(c) and (d). Different from the spiral pattern before the flow wave initiation (Fig. 19(a)), the wave lengths of the chemical waves are almost constant (about 1 mm) in the phase of flow wave propagation (see Figs. 19(c) and (d)). Coherence of the wavelength seems to be a primary factor for induction of the flow waves.

Next, we demonstrate a synchrony between the oscillatory flow velocity and flow waves. Figure 20 shows space-time plots of chemical activity modified by flow waves and oscillatory flow velocity induced in three types of spiral core systems:

1) one spiral pair (OSP1) system with a spiral center near the left boundary of the dish (same as in Fig. 15),

2) one spiral pair (OSP2) system with a spiral center at the middle of the Petri dish,

3) two spiral pair (TSPs) systems with two spiral centers located symmetrically in the right and the left half of the Petri dish (same as in Fig. 16).

A temporal development of the respective chemical activity is visualized along the centerline as shown by dotted lines in the upper row of pictures in Figs. 20(a)–(c). In the lower pictures of Fig. 20, a faint periodic structure appears (see arrowed patterns), which indicates a modified pattern induced by flow waves. Flow waves propagate with almost constant velocity and annihilate at the spiral center. The velocities of flow waves in OSP1 (a) and OSP2 (b) systems were 2.5 mm/s and 0.92 mm/s, respectively. The period of flow waves was about 40 s in both systems. Image sequences of the flow oscillations measured simultaneously at the surface are superimposed on the space-time plot of the respective chemical activities. We can recognize synchronization between oscillatory flow (white solid line) and periodic pattern modification (faint periodic structure) caused by flow waves.

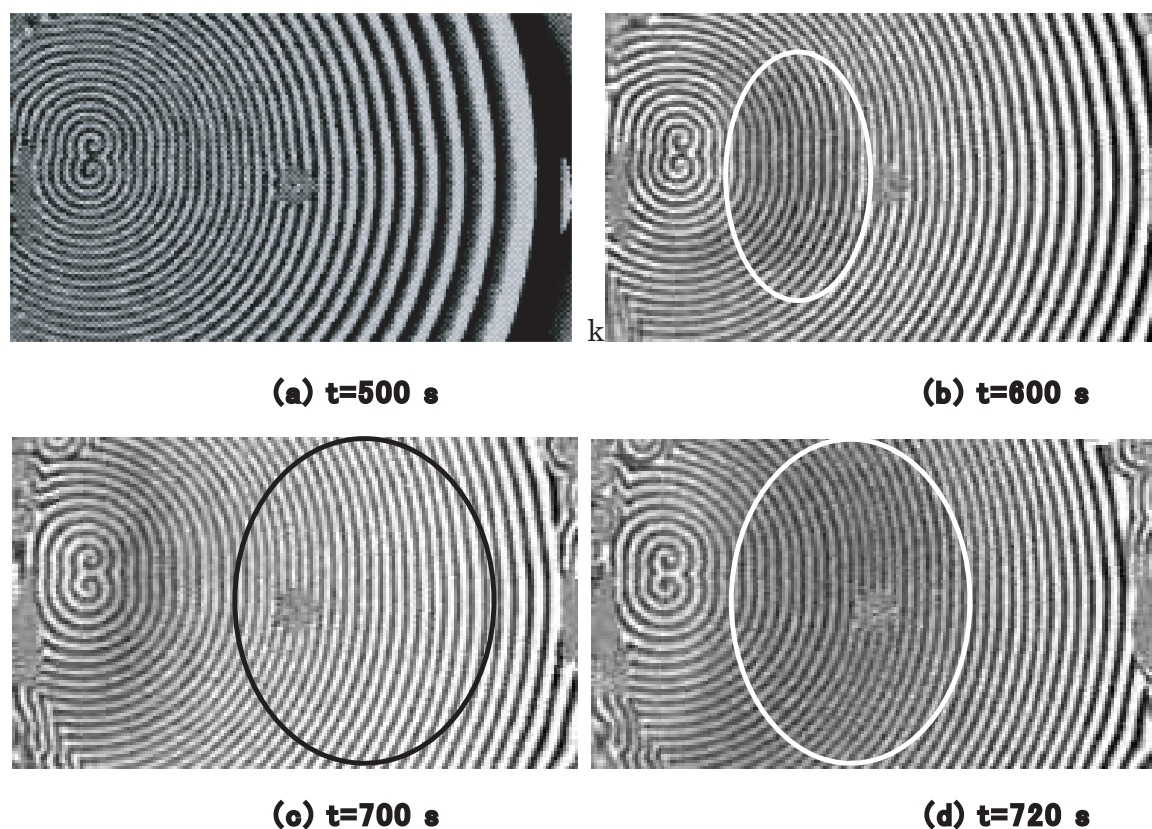We also noticed the propagation of flow waves in the

Fig. 19. Initiation and propagation of flow waves induced in a thin BZ-solution layer after exciting a chemical spiral wave train (Miike *et al.*, 2010). (a) Before initiation of flow waves, (b) just after flow wave initiation. Images (c) and (d) show the phase of flow waves with a brighter profile (c) and a darker one (d). The flow waves were initiated at the right boundary of the dish and propagated toward the core of the spiral waves. The white ellipse contains the darker profile area of the flow waves, while the black ellipse shows the brighter one, which corresponds to the white band in Fig. 18(A).

TSPs system having two spiral centers (see **A** and **B** in the upper picture of Fig. 20(c)). The lower figure in Fig. 20(c) indicates that flow waves are initiated at the collision line of the two spiral patterns and propagate toward the respective centers of the two spiral centers. These flow waves switched their propagation direction every 30 s, e.g., from the collision line to center **A** and from this line to the other center **B**. The velocity of flow waves is 1.25 mm/s. A temporal trace of the velocity of surface flow is superimposed onto the spatiotemporal pattern of chemical waves (see lower image in Fig. 20(c)). The superimposed pattern indicates a fine synchrony between flow waves propagation and oscillatory surface flow. Thus, the periodic change of oscillatory surface flow can be understood as being due to the periodic passage of flow waves.

4.3 Global synchrony of flow oscillator associated with chemical wave train

In Subsection 4.2, we discussed the global structure of the CDCs appearing in a thin BZ-solution layer. Especially, coherent patterns of chemical spiral waves correlated with self-organized convective flow oscillation were described. The synchronization of the flow oscillations brought about a global pattern dynamics of flow waves in the solution layer. We understand that the oscillatory flow (observed at a point) corresponds to the periodic passage of flow waves (observed globally). In all three types of spiral wave systems (see Fig. 20), flow waves propagated from the boundaries to the center of the spiral waves. In this section, we focus on the "spiral flow wave".

At the beginning, a pair of chemical spiral waves was initiated at the middle of a large Petri dish (100 mm diameter). The spiral pattern rotated with a period of about 18 s and became the source of a chemical wave train, which propagated from the middle to the boundary of the Petri dish with a minimum wavelength of about 1 mm. Then, 12 min after the spiral pattern was initiated, an outwardly rotating flow wave (spiral flow wave) appeared spontaneously (Sakurai *et al.*, 2003; Mahara *et al.*, 2009). Time sequences of the rotating flow wave are shown in Fig. 21. The tip of the spiral flow wave was located near the chemical spiral pair. This spiral flow wave had a period of about 30 s and continued for 30 min after the spiral pair had been initiated.

Figure 22 shows another example of the spiral flow wave. Here, the direction of the observed surface flows at three points was overlaid on the time sequence of the spiral flow wave. The surface flow was always streaming, i.e., the velocity of the surface flow was always nonzero, and the directions of the surface flow rotated continuously. This rotation had the same period as the spiral flow wave and was synchronized with the spiral flow wave pattern. When the flow wave pattern passed the observation points, which are shown by the white dots in the respective image in Fig. 22, surface flows were directed almost inward, i.e., toward the center of the dish (see Figs. 22(b-1) and (c-4)). On the contrary, when the flow wave pattern was located at the opposite side of the observation points, the surface
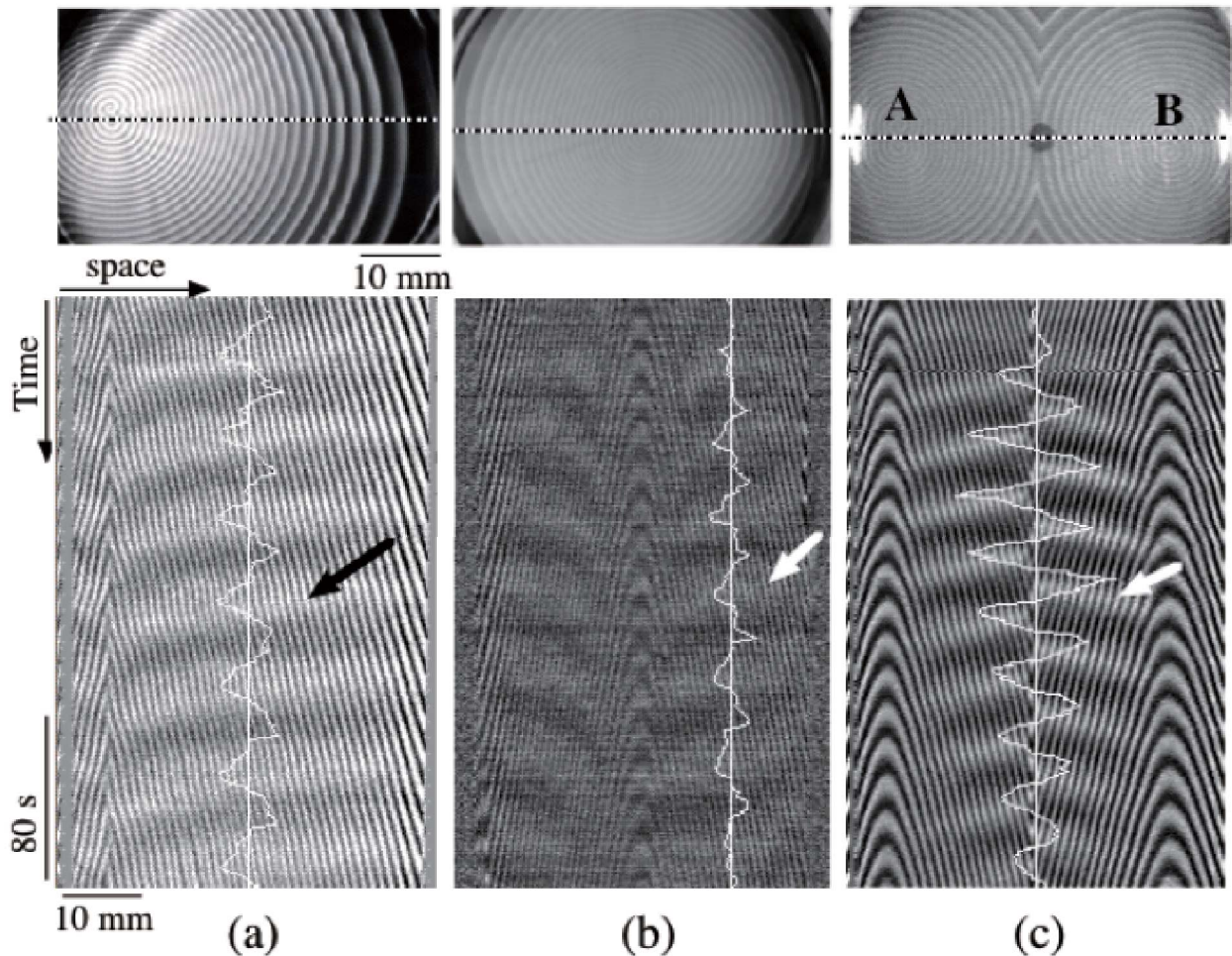
Fig. 20. Space-time plot of chemical activity modified by oscillatory flow induced in three types of spiral systems (Sakurai *et al.*, 2004). The white lines superimposed on the space-time plot correspond to the flow velocity development in Fig. 15. The line plotted in (b) is the velocity measured between the spiral center and the boundary of petri dish. (a) OSP1 system. (b) OSP2 system. (c) TSPs system.

flows were directed outward (see Figs. 22(b-3) and (c-2)). Such macroscopic propagation of a spiral-shaped flow wave (wavelength about 50 mm) was induced spontaneously in the preexisting *reaction-diffusion* structure of chemical spiral waves (wavelength about 1 mm). The shape of spiral flow wave is also synchronized with the direction of surface flow. Thus, the pattern dynamics links two different hierarchical levels of pattern formation, i.e., those of chemical and flow waves in a *reaction-diffusion-convection* system.

Figure 23 shows surface deformations of the rotating flow wave (Mahara *et al.*, 2009). These surface deformations are based on the fringe patterns captured by a Fizeau interferometer (Okada *et al.*, 2007). The global surface tilt was certainly not due to tilting of the Petri dish with respect to the ground. The vertical distance between the highest and lowest levels is about 3 μm. The normal vector of the tilting surface rotated with a period of about 30 s, the same as that of the rotating flow wave (Mahara *et al.*, 2009). Figure 24 provides a scheme of the dynamics of the spiral flow wave synchronized with rotational surface deformation and flow direction change. We observed simultaneously the surface flow directions and the surface deformation of the rotating flow wave by use of two observation methods (Fizeau in-

terferometer and microscope video imaging system). From the results of these observations, we determined the surface flow structure of the rotating flow wave. The normal vector of the tilting surface rotated also with a period of about 30 s. Thus, the structure was synchronized with the flow wave pattern, and had a larger scale (about 50 mm) than the chemical wavelength (about 1 mm).

Several important facts that we found to understand the mechanism of the oscillatory flow induced in the BZ solution by propagating spiral waves are summarized as.

1) Global flow waves induced in the BZ-solution under exciting one spiral pair (OSP) at the boundary (see Fig. 20(a)) or at the middle of the dish (see Fig. 20(b)) (Matthiessen and Müller, 1995). The flow waves propagate towards the center of the spiral pattern, where they finally disappear.

2) Switching flow waves by exciting two spiral pairs (TSPs) symmetrically (see Fig. 20(c)). The flow waves propagate alternately toward the left and the right center of the respective spiral waves (Sakurai *et al.*, 1997b, 2004).

3) Circular or spiral-shaped flow waves induced by exciting spiral pairs at the middle of the Petri dish (Sakurai *et al.*, 2003). Under a specific condition, flow waves are induced
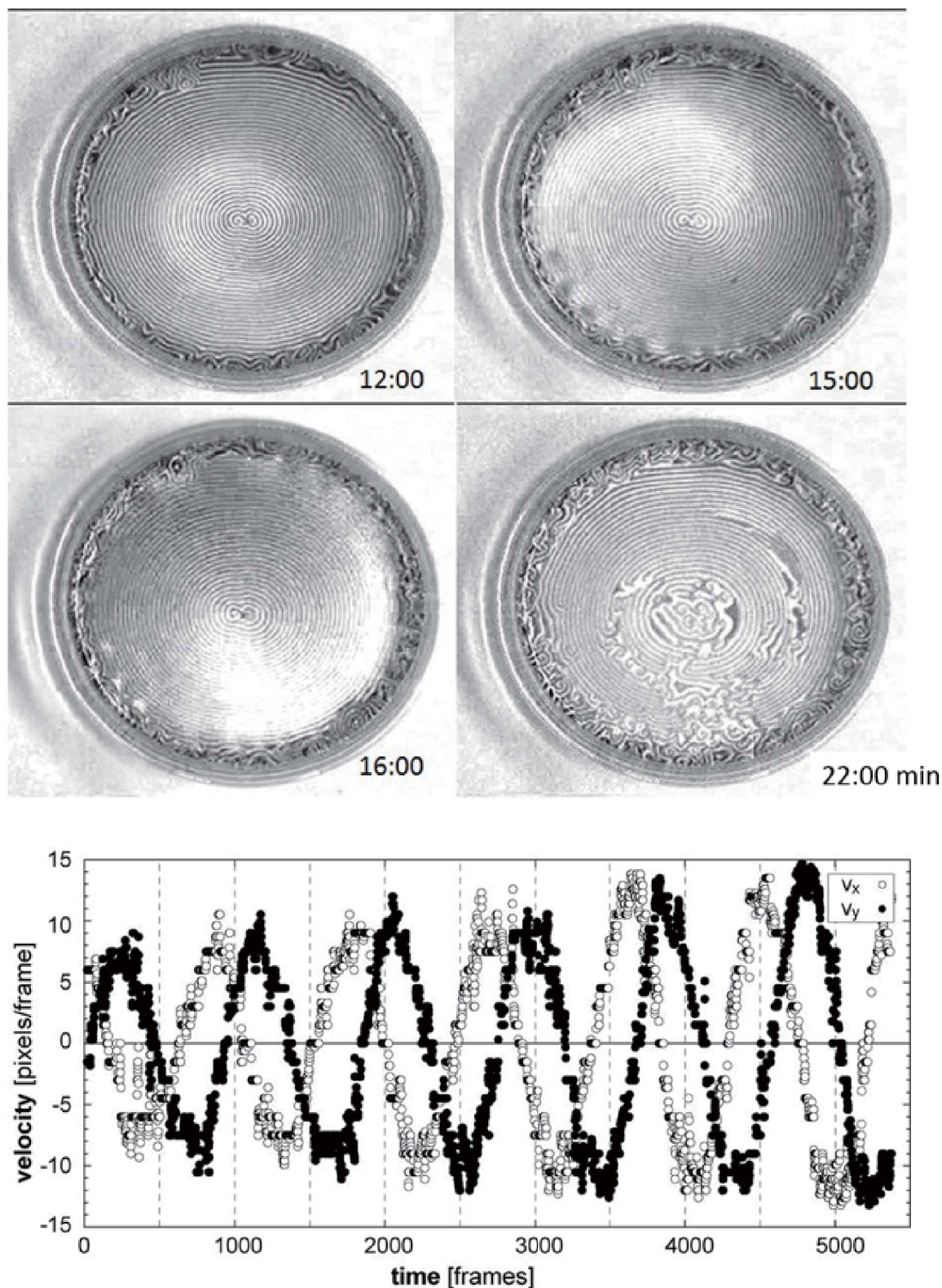
Fig. 21. Time series of a spiral flow wave (top 4 pictures). A chemical spiral pair was triggered at the middle of the dish ($t = 0 : 00$ min). Other than in Fig. 20, the spiral-shaped flow wave started from the chemical spiral pair ($t = 12 : 00$ min) and propagated in outward direction. A rotating surface flow was accompanied by the flow wave. The surface flow did not stabilize to a motionless state but grew in amplitude (see the bottom figure sampled by 30 Hz: 1 s = 30 frames) until the system is self-collapsed ($t = 22 : 00$ min) (Miike *et al.*, 2010). The top pictures are obtained by image processing, which is based on a new pixel-based temporal brightness enhancement (Otaka *et al.*, 2013).
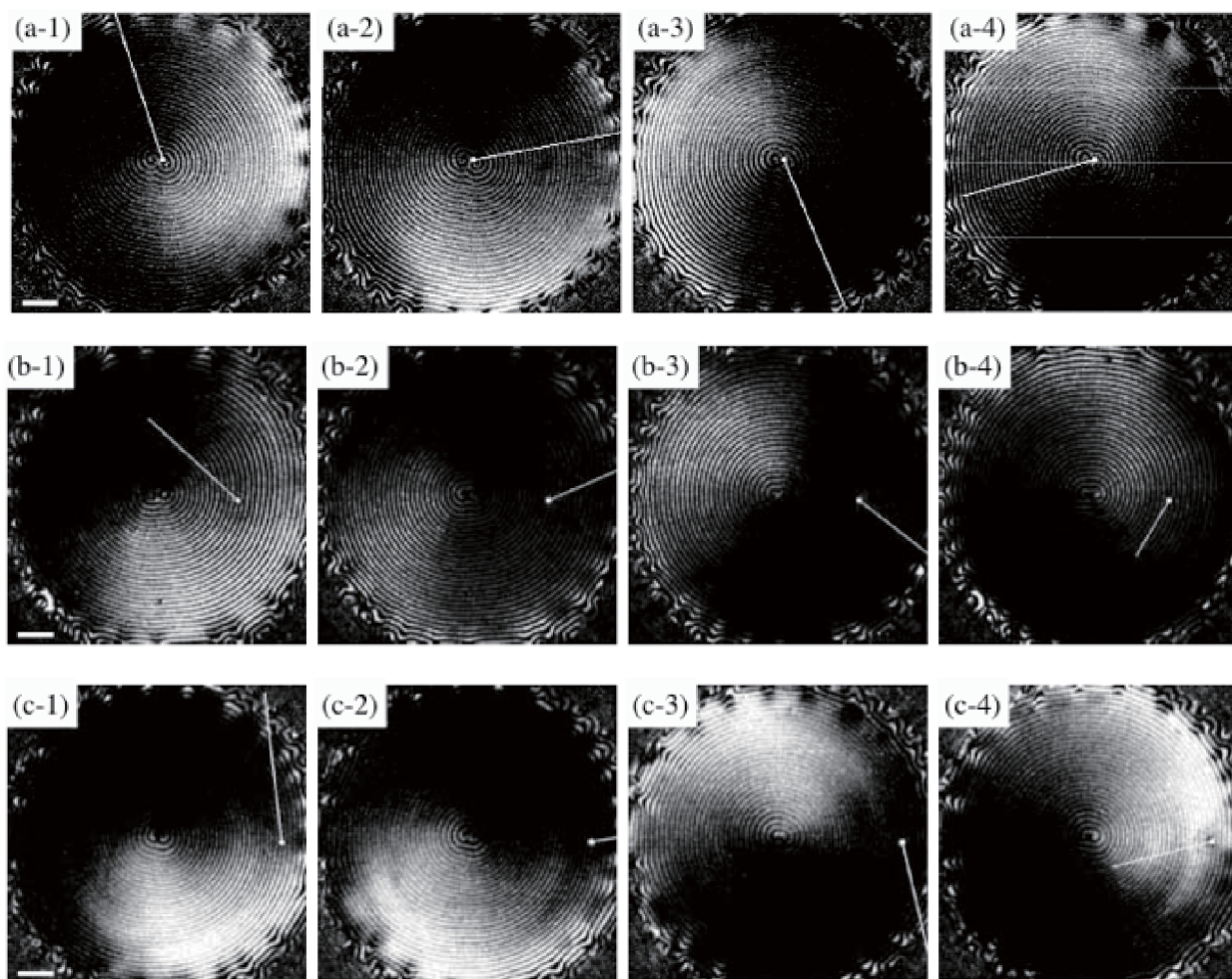
Fig. 22. Time sequences of a spiral flow wave with indication of the direction of surface flow (Mahara *et al.*, 2009). Pattern contrasts are emphasized so that only the flow wave pattern appears as a brighter area. The white dots in the respective pictures show observation points of the surface flow. The white lines indicate the direction of flow at the observation points; (a) $r = 0$ mm, (b) $r = 33$ mm, and (c) $r = 66$ mm, where r is the distance between the particular observation points and the chemical spiral center. The time interval is about 8 s. Scale bar in (a-1), (b-1), and (c-1): 10 mm.

around the center of the spiral waves and propagate toward the periphery of the Petri dish.

5. Evolutionary Pattern Dynamics

5.1 Self-organized successive transitions induced by CDCs

As described in the preceding sections, complex pattern dynamics emerging in the BZ-solution are accompanied by a large variety of convective effects induced by chemical activities. Here, we try to understand the mutual relationships in this variety of chemically driven convections (CDCs). A slightly different condition of the solution preparation produces a pronounced difference of spatiotemporal pattern dynamics in the system. These are single chemical waves propagating with constant velocity, accelerating propagation of the big wave, and rotating spiral waves. All of these dynamics are accompanied by a variety of CDCs.

Under well-controlled conditions of the BZ-solution and that of the container (Petri dish), we can observe a successive transition starting from the propagation of a single triggered chemical wave to that of the big wave and, finally, to spiral waves accompanied by oscillatory convection or to spiral-shaped flow waves with rotating flow direction (see

Fig. 1) (Miike *et al.*, 1992). A variety of spatiotemporal pattern dynamics emerges by only triggering a single chemical wave in the dish. A requirement is to have a clean and a quiet condition of excitable BZ-solution to realize the successive transitions. Consequently, spontaneous excitation of uncontrolled chemical wave must be suppressed during the successive transitions that continue for more than 15 minutes.

Figure 25 shows another example of the successive transition of CDCs in chemical pattern dynamics from the big wave to well-developed spiral waves. Discrete propagation of chemical waves results in a large velocity amplitude (more than 100 μm/s) of oscillatory convection having a long oscillation period (more than 2 minutes). If this velocity exceeds the propagation velocity of ordinary chemical waves (about 100 μm/s), the chemical wave front is disrupted by the convection and falls apart into small pieces of chemical waves, which subsequently leads to spontaneous development of spiral waves. Since spiral waves have short period of oscillation, the amplitude of the convection decreases with time (see Fig. 25: 5–10 minutes). Finally, a well-developed global structure of spiral waves induces the oscillatory flow having a short oscillation period (about 40
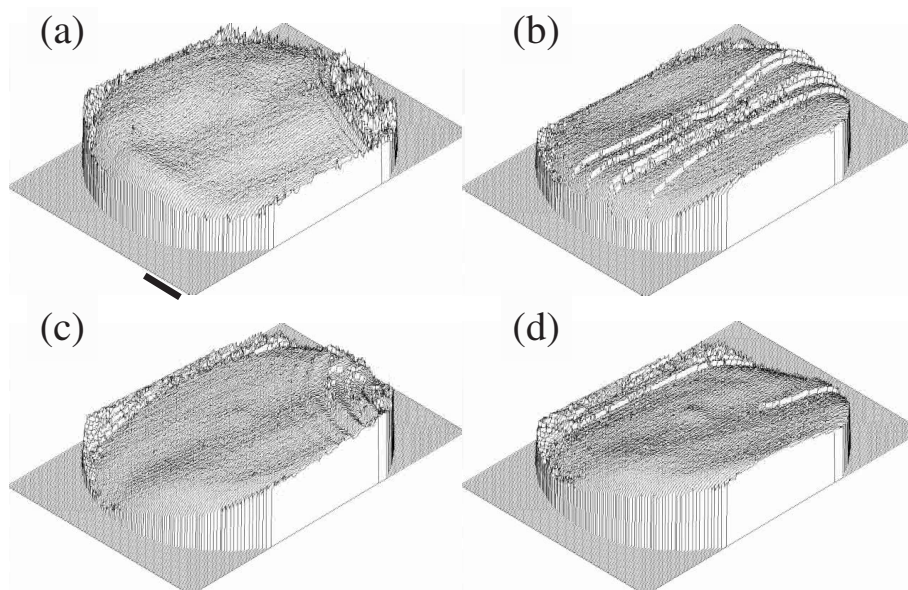
Fig. 23. Time series of analyzed surface deformation. The observation area is a circular region with a radius of 60 mm. The time interval between the
3D-plots is about 7.5 s. Scale bar in (a) is 10 mm (Mahara *et al.*, 2009).
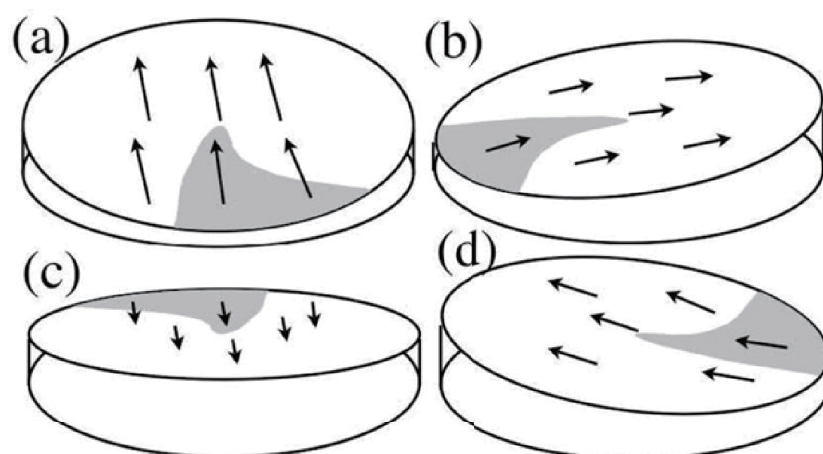

Fig. 24. Schematic presentation of the time evolution of surface flow structure and surface deformation, as observed during the rotating spiral flow
developed in a thin solution layer of the BZ-reaction. A chemical spiral core was excited at the middle of the Petri dish (Mahara *et al.*, 2009). The
global structure of surface flows is determined from chemical wave pattern contrast and surface flow direction in Fig. 22.

seconds), about 14 minutes after triggering the single chem-
ical wave. Consequently, triggering a single wave leads to
the onset of a well-developed coherent chemical spiral pat-
tern and oscillatory convection, which represents a global
synchronization of hydrodynamic local oscillators associ-
ated with the respective chemical wave train.

5.2 Evolutionary pattern dynamics in a reaction-diffusion-convection system

Since the BZ-solution in a Petri dish is a batch reactor, the
system conditions (chemical activity) are changing through
chemical wave initiation and propagation. The major mech-
anism to induce the convection is based on the Marangoni
instability caused by a concentration gradient of chemical
materials (Matthiessen *et al.*, 1996). The gradient is re-
lated to self-organized action by the development of spi-
ral structures in the batch reactor producing periodic and
tightly spaced concentration gradients in the reactor. Be-

cause of the slow propagation velocity of the waves, the
core region of the spiral structure repeats many oscillations
compared to the peripheral region of the spiral (see Figs.
15(a), (b), and (c)). Thus, a concentration gradient of the
reaction products like bromomalonic acid (BrMA) is estab-
lished in a self-organized way in the course of time. The
formation of such a gradient can be the origin of the CDCs
in the developed chemical spiral pattern. On the other hand,
as pointed out by Inomoto *et al.* (2000), the BrMA concen-
tration is a key control parameter to induce the big wave
propagation. They found that the surface tension decreases
with increment of BrMA concentration. Even single chem-
ical wave propagation causes a slight increment of BrMA
concentration in the solution layer, which may explain the
spontaneous induction of the big wave (see Fig. 1 (8:00))
after the propagation of the first circular wave.

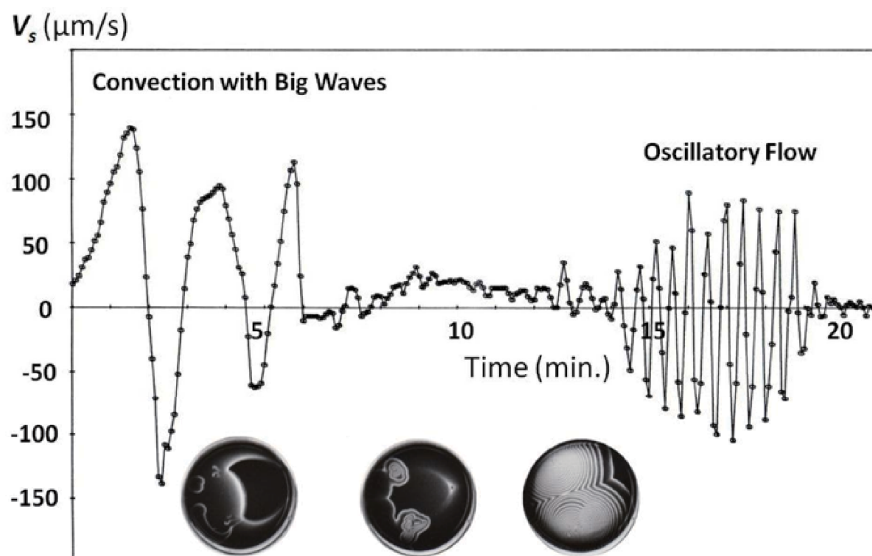The induction of the big wave leads to the successive dy-

Fig. 25. Convective pattern dynamics caused by a transition from discrete propagation of a chemical wave (like the big wave) to spiral waves (Miike and Sakurai, 2003). The oscillatory flow was induced spontaneously at around $t = 14$ min after triggering a single chemical wave ($t = 0$) in a thin solution layer of the BZ-reaction. The pictures at the bottom are the corresponding patterns.

namics of CDCs (see the oscillatory flow in Fig. 25: after 14 minutes). The oscillatory flow may contribute to an effective mixing of the solution layer to reduce the local non-uniformity of reactants such as malonic acid (MA) in the BZ-reaction. This effective mixing guarantees local openness of the system. In spite of the batch condition of the reactor, our system is not closed but open locally by receiving the reactant continuously from the solution layer itself. Since the reactant concentration is high enough, we can assume the existence of a reservoir which supplies enough reactant in the batch reactor. An important point is the rate of supply of the reactant from this reservoir. The supply is usually realized by molecular diffusion; however, the occurrence of the oscillatory flow contributes to establish a more effective supply from the peripheral region of the chemical pattern. Thus, the rate of supply or the degree of non-equilibrium changes suddenly by the occurrence of flow waves. In our batch reactor, it takes about 10 minutes to induce the oscillatory flow under the excitation of a chemical spiral structure. The system conditions may change in the course of time with the development of the structure. All of these functions are self-organized by CDCs induced in the thin solution layer with an open surface. Consequently, the successive pattern formations and accompanying convections (see Figs. 1 and 25) show a typical example of evolutionary and/or evanescent pattern dynamics, which appears in the batch reactor of a *reaction-diffusion-convection* system.

6. Discussion and Conclusion
6.1 Mechanism to establish CDCs in the BZ reaction
The first point of discussion is the mechanism of the described CDCs. Previous approaches for the CDCs adopted a numerical model in which appropriate reaction-diffusion equations and the Navier-Stokes equations with Marangoni effects were coupled. The first successful work was re-ported by Matthiessen *et al.* (1996) with a modified Orego-nator model determining the reaction-diffusion equations. These authors took into account both the gravity effect (buoyancy driven case) and Marangoni effect (surface-tension driven case) due to the concentration distributions of chemical species (activator and inhibitor). They clarified that the Marangoni-type convection linked to the inhibitor concentration yields the best fit to the experimental data of the vertical profile of the horizontal flow velocity distribution (see Fig. 14). The result is believed to be a reliable clue to understand the CDCs induced by chemical waves in the BZ-solution.

The second reliable report was proposed by Diewald *et al.* (1996) with a simple model similar to the one by Matthiessen *et al.* (1996) to present the oscillatory flow in chemically driven convection. They observed numerically a strong surface flow in the direction opposite to the propagation direction of the reaction fronts that can be traced back to the sharp fronts in the ferriin concentration which develop only when the reaction fronts are tightly spaced. They also suggested (Diewald *et al.*, 1996): "*An important observation from the simulation is the strong distortion of the reaction front near the surface. The reaction front gets disconnected from the free surface and the lateral gradients in the ferriin concentrations are smoothed out. The hydro-dynamic flows have thus lost their driving power and therefore the layer can relax to a motionless state. The disrupted reaction front will reconnect to the free surface and reestablish the strong gradients in the inhibitor (ferriin) concentration along the open surface, once the strong flow has relaxed to a motionless state. Clearly, this starts over the whole dynamics*". Our understanding of their explanation is as follows (Miike *et al.*, 2010). The strong surface flow in the direction opposite to the wave propagation disconnects the reaction front from the free surface and brings about a motionless state, which reconnects the reaction front to the
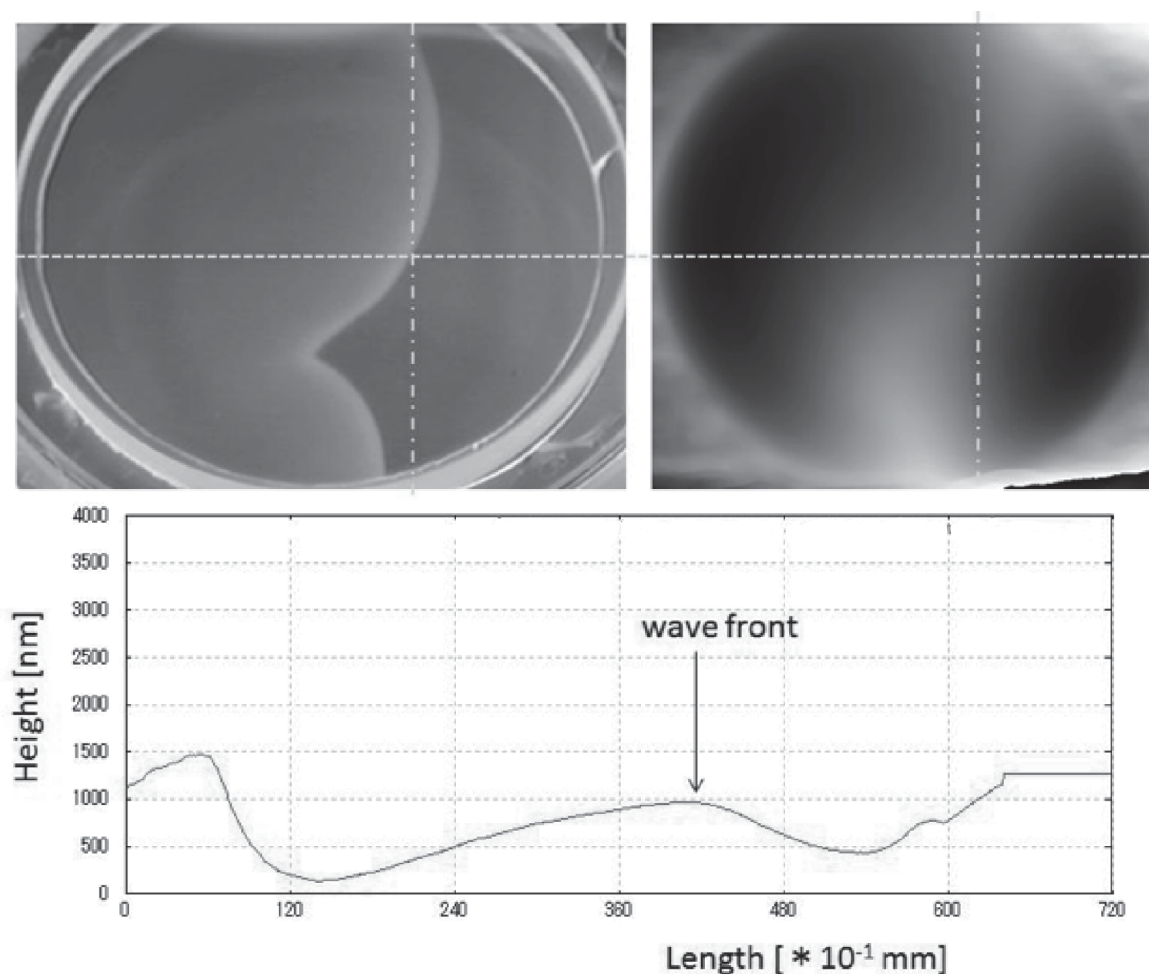
Fig. 26. Deformation of an air-liquid interface induced by CDC in a thin solution layer of the BZ-reaction (Okada *et al.*, 2007). The upper left figure shows the propagation of circular waves in a Petri dish, the upper right one a result of surface deformation analysis from a fringe pattern of a Fizeau interferometer. The lower figure shows a cross section of the surface deformation along the broken line in the upper figures.

free surface. This disconnection and reconnection mechanism is a key feature of their model. Once the strong hydrodynamic flow has developed, the flow disrupts the reaction front and within a short time the hydrodynamic flow stops. This picture may explain the oscillatory flow and propagating flow waves observed in a real system. However, the picture does not allow a continuous stream of the surface flow. The flow is expected to repeat a rapidly moving state and a motionless state via the connection and reconnection mechanism. Consequently, the model cannot explain the spiral flow wave having a continuous stream of hydrodynamic flow with growing amplitude (Miike *et al.*, 2010) and rotating flow direction (see Figs. 21 and 22). Although these approaches were partially successful in simulating the fluid flow observed in the laboratory experiments of the BZ-reaction (see Fig. 14), they do not provide a full understanding yet.

There are other activities related to CDCs in BZ-solution: Rossi *et al.* found chemical concentration waves segmented in the BZ reaction system (Rossi *et al.*, 2009), and performed a corresponding numerical simulation with gravity and Marangoni effects (Rossi *et al.*, 2012). Rongy *et al.* focused on the front of a chemical concentration

wave propagating in a shallow layer of a chemical solution, and performed numerical simulations based on the solutal Marangoni effect under a variety of thicknesses of the solution layer without the gravity effect (Rongy and De Wit, 2007). They confirmed the dependence of a traveling speed on thickness; the speed increases with the thickness of the solution. These numerical results were performed for the situation of propagating chemical reaction wave(s) in a thick solution layer of more than 1 mm. Thus, the details will not be considered here.

As discussed above, no reliable model has been proposed yet to explain the CDCs induced in the thin solution layer of BZ reagent with an open surface. Every experimental result requires a revision of the ordinary *reaction-diffusion-convection* model. Particularly, in the proposed models, the effect of surface deformation accompanied by the CDCs was not taken into account. Figure 26 shows an example of observed surface deformation induced by a circular chemical wave. Apparently, the deformation has a broad expansion in the dish. This global structure of the deformation may cause a quick response of the convection induced by the chemical wave (see Fig. 7). Since the layer depth is small enough (less than 1 mm), the CDC is caused

mainly by a surface-tension driven force. The deformation observed is very small (of the order of 1 μm). However, the broad structure of the deformation may contribute to the long-wavelength Marangoni instability (VanHook *et al.*, 1995; Boos and Thess, 1999; Or *et al.*, 1999) occurring in a very thin layer.

6.2 Hierarchical pattern dynamics establishing flow waves

The second point of discussion is the hierarchical structure of flow waves and self-organized waves in the thin layer of the BZ reaction. In particular, the emergence of spiral flow waves under the excitation of chemical spiral structures at the middle of the dish is remarkable. As discussed above, the disconnection and reconnection mechanism (Diewald *et al.*, 1996) between the reaction front and the free surface is not the universal model to induce the flow wave structure. Especially, in the case of the spiral flow wave, the induced flow never stops but is nourished by a continuous hydrodynamic flux with growing amplitude and rotating direction of the flow (see Fig. 21). It seems to be difficult to explain the hierarchical dynamics within the framework of an ordinary *reaction-diffusion-convection* approach. Consequently, one has to consider a modified approach. However, none of the proposed models has yet a sufficient capacity to explain the temporal development of CDCs and flow wave structure emerging in the real *reaction-diffusion-convection* systems.

Taking the non-stationary property of the batch reactor into account, problems of the proposed models, including our approach, may be the following:

1) The ordinary numerical model assumes a constancy of the system. For example, the model assumes that the reactant MA is available in sufficient amounts, and the concentration change of the product BrMA is negligible in the system. Namely, the concentrations of reactant MA and product BrMA are assumed to be constant.

2) Based on the assumption of the system's constancy, a local uniformness of the reactants and products is also assumed in the model.

In the real experiments, however, the constancy and the uniformness of the system are broken by the initiation of chemical waves. For instance, once a chemical rotor (spiral core) is excited in the middle of the dish under a well reduced condition of the BZ reagent, the uniformness of the reagent is lost gradually in the course of time. Rapid rotation period (about 18 s) and slow propagation velocity (about 0.1 mm/s) of the spiral wave enhances the non-uniformness of the system. It takes about 500 s for the chemical wave to reach the boundary of the dish, when we use a Petri dish with 10 cm diameter. During this time interval, the chemical oscillation is repeated more than 25 times by the chemical rotor. The enhanced non-uniformness or symmetry-breaking may establish a local gradient of reactants and products, which is a candidate for the Marangoni instability. This kind of self-organized non-uniformness in the batch reactor is not taken into account in the common model approaches.

The other possibility to induce flow waves is the well-established coherence of the chemical wave train. As clearly demonstrated in Figs. 19(b) and 21 (*t* = 12:00), the

lengths of the waves became almost constant just before the flow waves emerged. The induction period is regarded as the duration to establish the uniform wavelength in the dish. On the other hand, the velocity distribution profile (see Fig. 14) suggests that the induced CDCs feedback to deform the shape of the chemical wave front. A vertically deformed wave front leads to a modulation of propagation velocity of the wave through the curvature effect (Keener and Tyson, 1986; Foerster *et al.*, 1988). The modulation brings the deformed front back to a straight front. Thus, a combination between the CDCs and the curvature effect of the wave establishes an oscillatory propagation velocity of the wave front. In fact, the oscillatory convection generates a quite different situation compared to the gel system. Not only at the chemical level but also at the hydrodynamic level, the system behaves as a set of nonlinear oscillators having different levels of hierarchy. This type of scenario could produce a new picture to explain the origin of flow waves. Consequently, the well-established coherence of the chemical wave train is a possible actor to induce a dynamic synchrony among the nonlinear oscillators (Strogatz, 2003; Miike *et al.*, 2010). A coherent group dynamics of the densely spaced nonlinear oscillators can be a clue to understand the hierarchical pattern dynamics observed in the *reaction-diffusion-convection* system.

6.3 Concluding remarks

In this article, we reviewed the recent development of experimental studies on chemically driven convections (CDCs) emerging in a thin solution layer of the BZ reaction. These are solitary wave-like convections and oscillatory or rotating convections, accompanied by flow waves due to the excitation of chemical waves. We also summarized previous models to explain the CDCs and pointed out several problems of these model descriptions. Based on the discussions in the previous sections, we summarize our conclusions:

1) The mechanism of CDCs induced in a thin solution layer of BZ-reaction is not yet well understood. Even in the simplest case of CDC induced by a single circular wave, no model has succeeded to establish the complete mechanism of the real phenomenon.

2) The observed spiral flow wave has added a new aspect to the phenomenon of flow waves. The flow structure is not oscillatory but rotating, and there is a continuous stream of surface flow with growing amplitude (Miike *et al.*, 2010) and rotating flow direction. The new picture is inconsistent with the previous model, in which the surface flow is expected to alternate between a rapidly moving state and motionless state via a connection and reconnection mechanism (Diewald *et al.*, 1996).

The above conclusions require a revision of the common *reaction-diffusion-convection* models. For this purpose, we propose several candidate mechanisms and new model assumptions. These are:

1) The effect of surface deformations accompanied by the CDCs should be considered in a revised and extended model.

2) In the real system, the constancy and the uniformness of the system are broken by the initiation of chemical waves. This kind of self-organized evolutional charac-

teristics of non-constancy and non-uniformness in a batch reactor should be taken into account.

3) A chemical wave train coupled with CDCs could be considered as a set of nonlinear oscillators having different levels of hierarchy. This model should provide a new scenario to explain the global flow waves inducing synchrony among the chemical waves through the oscillatory convection and wave front modulation by the curvature effect. In particular, we wish to emphasize the role of synchrony among propagating nonlinear oscillators to establish hierarchical pattern dynamics of chemical wave trains and flow waves. However, the mechanisms to realize these coherences and/or synchronies of hydrodynamic patterns are not well established yet at the present stage.

On the other hand, we have demonstrated typical examples (see Figs. 1 and 25) of evolutional pattern dynamics induced by CDCs in a batch reactor. The system conditions of the batch BZ-solution are changing with time. The system is not in a stationary state; however, emerging phenomena in the system show a temporal development of pattern dynamics. The direction of the development is from simple to complex, which looks like an evolution and/or an evanescence emerging in a real system determined by the coupling of *reaction, diffusion, and convection.*

References

Agladze, K., Krinsky, V. I. and Pertsov, A. M. (1984) *Nature*, **308**, 834–835.

Boos, W. and Thess, A. (1999) *Phys. Fluids*, **11**, 1484–1494.

Borckmans, P. and Dewel, G. (1988) Chemical structures and convection, in *From Chemical to Biological Organization* (eds. M. Markus, S. C. Müller and G. Nicolis), pp. 114–121, Springer Series in Synergetics 39, Springer, Berlin.

Castets, V., Dulos, E., Boissonade, J. and De Kepper, P. (1990) *Phys. Rev. Lett.*, **64**, 2953–2956.

De Kepper, P., Castets, V. and Boissonade, J. (1991) *Physica D*, **49**, 161–169.

Diewald, M., Matthiessen, K., Müller, S. C. and Brand, H. R. (1996) *Phys. Rev. Lett.*, **77**, 4466–4469.

Field, R. J. and Burger, M. (1985) *Oscillations and Travelling Waves in Chemical Systems*, Wiley, New York.

Foerster, P., Müller, S. C. and Hess, B. (1988) *Science*, **241**, 685–687.

Hashimoto, H., Müller, S. C. and Miike, H. (1991) *Bussei-Kenkyu (Kyoto University)*, **56**(2), 252–254 (in Japanese).

Inomoto, O., Abe, K., Amemiya, T., Yamaguchi, T. and Kai, S. (2000) *Phys. Rev. E*, **61**, 5326–5329.

Kai, S., Ariyoshi, T., Inenaga, S. and Miike, H. (1993) *Physica D*, **84**, 269–275.

Kapral, R. and Showalter, K. (1994) *Chemical Waves and Patterns*, Kluwer, Dordrecht.

Keener, J. P. and Tyson, J. J. (1986) *Physica D*, **21**, 307–324.

Kuramoto, Y. and Haken, H. (1980) *Dynamics of Synergetic Systems*, Springer Series in Synergetics.

Mahara, H., Okada, K., Nomura, A., Miike, H. and Sakurai, T. (2009) *Phys. Rev. E*, **80**, 015306(R)1-4.

Matthiessen, K. and Müller, S. C. (1995) *Phys. Rev. E*, **52**, 492–495.

Matthiessen, K., Wilke, H. and Müller, S. C. (1996) *Phys. Rev. E*, **53**, 6056–6060.

Miike, H. and Müller, S. C. (1990) Chemical pattern dynamics by chemically induced hydrodynamic flow, in *Nonlinear Evolution of Spatio-temporal Structures in Dissipative Continuous Systems* (eds. F. H. Busse and L. Kramer), Plenum Press, New York, *NATO ASI Series B: Physics*, **225**, 293–297.

Miike, H. and Sakurai, T. (2003) *Forma*, **18**, 197–219.

Miike, H., Koga, K., Momota, M. and Hashimoto, H. (1987) *Jpn. J. Appl. Phys.*, **26**, L1431–L1434.

Miike, H., Müller, S. C. and Hess, B. (1988) *Chem. Phys. Lett.*, **144**, 515–520; *Phys. Rev. Lett.*, **61** (1988), 2109–2112; *Phys. Lett. A*, **141** (1989), 25–30.

Miike, H., Yamamoto, H. and Momota, M. (1992) Hydrodynamic effects induced by chemical wave propagation, in *Pattern Formation in Complex Dissipative Systems* (ed. S. Kai), pp. 191–200, World Scientific.

Miike, H., Yamamoto, H., Kai, S. and Müller, S. C. (1993) *Phys. Rev. E*, **48**, R1627–R1630.

Miike, H., Zhang, L., Sakurai, T. and Yamada, H. (1999) *Patt. Recog. Lett.*, **20**, 451–461.

Miike, H., Miura, K., Nomura, A. and Sakurai, T. (2010) *Physica D*, **239**, 808–818.

Müller, S. C., Plesser, Th. and Hess, B. (1985) *Analytical Biochemistry*, **146**, 125–133.

Okada, K., Yokoyama, E. and Miike, H. (2007) *Electron. Comm. Jpn. Part 2*, **90**, 61–73.

Or, A. C., Kelly, R. E., Cortelezzi, L. and Speyer, J. L. (1999) *J. Fluid Mech.*, **387**, 321–341.

Otaka, K., Osa, A., Miike, H. and Okada, K. (2013) Motion visualization using an impulse response model in human vision, in *Proceedings of "Spatio-temporal Organization in Non-equilibrium Systems"* (23rd February, 2013, Fukuoka, Japan), 063.

Pojman, J. A. and Epstein, I. R. (1990) *J. Phys. Chem.*, **94**, 161–169.

Pojman, J. A., Nagi, I. P. and Epstein, I. R. (1991) *J. Phys. Chem.*, **95**, 1306–1311.

Rongy, L. and De Wit, A. (2007) *J. Eng. Math.*, **59**(2), 221–227.

Rossi, F., Liria, M. and Liveri, T. (2009) *Ecol. Model.*, **220**, 1857–1864.

Rossi, F., Budorini, M. A., Marchettini, N. and Carballido-Landeira, J. (2012) *Chaos*, **22**(3), 037109 (11 pages).

Sakurai, T., Yokoyama, E. and Miike, H. (1997a) *Phys. Rev. E*, **56**, R2367–R2370.

Sakurai, T., Miike, H., Yokoyama, E. and Müller, S. C. (1997b) *J. Phys. Soc. Jpn.*, **66**, 518–521.

Sakurai, T., Miike, H., Okada, K. and Müller, S. C. (2003) *J. Phys. Soc. Jpn.*, **72**, 2177–2180.

Sakurai, T., Inomoto, O., Miike, H. and Kai, S. (2004) *J. Phys. Soc. Jpn.*, **73**, 485–490.

Strogatz, S. (2003) *SYNC: The Emerging Science of Spontaneous Order*, New York.

VanHook, S. J., Schatz, M. F., McCormick, W. D., Swift, J. B. and Swinney, H. L. (1995) *Phys. Rev. Lett.*, **75**, 4397–4400.

Winfree, A. (1987) *When Time Breaks Down: The Three-dimensional Dynamics of Electrochemical Waves and Cardiac Arrhythmias*, Princeton University Press.

Yoshikawa, K., Kusumi, T., Ukitsu, M. and Nakata, S. (1993) *Chem. Phys. Lett.*, **211**, 211–213.